Segmentation and Disruption of the East Pacific Rise in the Mouth of the Gulf of California

PETER LONSDALE

Scripps Institution of Oceanography, University of California, San Diego, La Jolla, USA

(Received 6 January, 1994; accepted 14 October, 1994)

Key words: Spreading centers, nontransform offsets, crustal rifting.

Abstract. Analysis of new multibeam bathymetry and all available magnetic data shows that the 340 km-long crest of the East Pacific Rise between Rivera and Tamayo transforms contains segments of both the Pacific-Rivera and the Pacific-North America plate boundaries. Another Pacific-North America spreading segment ("Alarcon Rise") extends 60 km further north to the Mexican continental margin. The Pacific-North America-Rivera triple junction is now of the RRR type, located on the risecrest 60 km south of Tamayo transform. Slow North America-Rivera rifting has ruptured the young lithosphere accreted to the east flank of the rise, and extends across the adjacent turbidite plain to the vicinity of the North America-Rivera Euler pole, which is located on the plate boundary. The present absolute motion of the Rivera microplate is an anticlockwise spin at 4° m.y.$^{-1}$ around a pole located near its southeast corner; its motion has recently changed as the driving forces applied to its margins have changed, especially with the evolution of the southern margin from a broad shear zone between Rivera and Mathematician microplates to a long Pacific-Rivera transform. Pleistocene rotations in spreading direction, by as much as 15° on the Pacific-Rivera boundary, have segmented the East Pacific Rise into a staircase of en echelon spreading axes, which overlap at lengthening and migrating nontransform offsets. The spreading segments vary greatly in risecrest geomorphology, including the full range of structural types found on other rises with intermediate spreading rates: axial rift valleys, split shield volcanoes, and axial ridges. Most offsets between the segments have migrated southward, but within the past 1 m.y. the largest of them (with 14–27 km of lateral displacement) have shown "dueling" behavior, with short-lived reversals in migration direction. Migration involves propagation of a spreading axis into abyssal hill terrain, which is deformed and uplifted while it occupies the broad shear zones between overlapping spreading axes. Tectonic rotation of the deformed crust occurs by bookshelf faulting, which generates teleseismically recorded strike-slip earthquakes. When reversals of migration direction occur, plateaus of rotated crust are shed onto the rise flanks.

Introduction

Study area

This paper concerns the risecrest accreted in the past 2.6 m.y. by the 400 km-long spreading center between the Rivera transform fault system and a sheared continental margin in the Gulf of California. It is traditionally considered part of the East Pacific Rise (EPR), though other names have been used to emphasize its isolation and distinctive geologic history, tectonic role, spreading rate and structure. Alternative names for the northernmost, continent-abutting segment, which has the large Alarcon Seamount on its west flank, include Alarcon Rise (Niemitz and Bischoff, 1981), Gulf Rise (Kastens *et al.*, 1979) and Pescadero Rift (Ness *et al.*, 1991). The multi-segmented rise south of Tamayo transform, where the axis was in contact with continental crust until just 1 m.y. ago, has been called Rivera Ridge and Rivera Rise by Ness *et al.*, (1981; 1991).

Oceanic crust accreted in this region before the end of Chron C2A (2.6 Ma) records the initiation of the Gulf of California, the abandonment and replacement of the first intercontinental spreading site at Maria Magdalena Rise, and initial stages in the replacement of Clarion transform by Rivera transform. These are topics for other papers, but because this history affects the structure of the present risecrest it is sketched in Figure 1. By 2.6 Ma, spreading had ceased at Maria Magdalena Rise, and Tamayo transform had acquired its present length. Slow east–west spreading between the Pacific plate and Mathematician microplate continued at the northernmost segments of the dying Mathematician Ridge (future sites of the volcanic islands of Socorro and San Benedicto), and had also prevailed further north for 1.5 m.y., at a 50 km-

Marine Geophysical Researches **17**: 323–359, 1995.

long spreading axis linked to Mathematician Ridge by the 70 km-long left-lateral Clarion strike-slip fault zone. This axis, which accreted a further 15 km-wide strip of crust after the end of Chron 2A, was also linked to the EPR axis at the eastern margin of the Mathematician microplate, by a broad zone of right-lateral shearing at the northern margin of the microplate. Soon after Chron 2n, following complete capture of Mathematician microplate by the Pacific plate, this long, diffuse shear zone evolved into Rivera transform, a typically narrow oceanic fault zone parallel to relative motion of the Pacific plate. The western end of this new transform had a more northwesterly strike than Clarion fracture zone, causing the slow-spreading rise segment immediately north of the fracture zone to be by-passed by the reconfigured plate boundary, and to become extinct.

The present spreading center north of Rivera transform is a hybrid, a conjunction of two different plate boundaries (Pacific-North America and Pacific-Rivera) along the crest of two different types of rise (an intercontinental mid-ocean ridge and an oceanic rise), with different histories but similar intermediate (52–68 mm yr^{-1}) spreading rates. The northern half originated in the past 5 m.y. by propagating through oceanic and continental lithosphere. It is now at the crest of a young mid-ocean ridge with turbidite-smothered flanks, built as Baja California (a continental block captured by the Pacific plate) moves away from the North American mainland (Figure 1). The southern half of the spreading center is a remnant of the rapidly opening Pacific-Farallon and Pacific-Cocos boundary that accreted most of the present floor of the North Pacific, and most of the lithosphere subducted at its eastern marginal trenches. The east flank of this oceanic rise now moves, according to McKenzie and Morgan (1969) and Atwater (1970), as an independent oceanic microplate (the Rivera plate), which is being slowly overridden by North America along its eastern boundary (de Mets and Stein, 1990). The Pacific-Rivera part of the EPR is a still-active example of the short-lived but rapidly evolving microplate boundaries that developed repeatedly during the past 30 m. y., as convergence of the EPR with the continental margin led to episodic detachment of plate fragments (microplates) from the rapidly subducting plates of the eastern rise flank (Lonsdale, 1991). The usual fate of these predecessors of the Rivera plate (e.g. the Monterey, Guadalupe and Magdalena plates), as shown by the festoon of abandoned Miocene risecrests west of the California and Baja California margins, has been capture by the Pacific plate after a few million years of slow to intermediate spreading along their western boundaries.

In some respects this is one of the most thoroughly investigated parts of the EPR. Larson (1972), Ness *et al.* (1981; 1991), and Lewis *et al.* (1983) reported systematic bathymetric and magnetic surveys of the entire width of the rise, partly designed to unravel the history of opening of the gulf and the relative motion of the Pacific and North American plates. Many subsequent transits of this well traveled region help fill in the 20–30 km-wide gaps in their survey grids and replace some of the older, poorly navigated tracklines, and were incorporated in recent syntheses by Lonsdale (1989a, 1991) and de Mets and Stein (1990). The convenient nearshore location of this part of the EPR crest has also attracted many detailed investigations of spreading center processes since the first near-bottom survey (Larson, 1971). Topics have included the width and structural subdivisions of the plate boundary zone (e.g. Normark, 1976; Francheteau *et al.*, 1981), the distribution of lava types and basalt chemistries (e.g. Ballard *et al.*, 1981; Juteau *et al.*, 1980; Bender *et al.*, 1984), convective cooling and precipitation of hydrothermal minerals (e.g. Spiess *et al.*, 1980; Goldfarb *et al.*, 1983; Alt *et al.*, 1987), the formation of abyssal hills and near-axis seamounts (e.g. Rangin and Francheteau, 1981; Macdonald and Luyendyk, 1985; Allen *et al.*, 1987), and the width of transition zones between magnetic stripes (Macdonald *et al.*, 1980; 1983). The fieldwork for these projects has been concentrated at the "RISE Area" near latitude 21° N. The largest lateral offset of the risecrest, the 70 km-long Tamayo transform fault, has also been surveyed (Kastens *et al.*, 1979), and examined with manned and unmanned submersibles (Macdonald *et al.*, 1979; Choukroune *et al.*, 1981; Gallo *et al.*, 1984).

Few studies in the mouth of the gulf have used multibeam bathymetry, a data type that has revolutionized description and understanding of the structural geomorphology of other Pacific rises, such as the Juan de Fuca Ridge (e.g. Karsten *et al.*, 1986) and fast-spreading parts of the EPR (e.g. Macdonald *et al.*, 1984; Lonsdale, 1989b). Some of the bathymetry collected in the RISE Area and around Tamayo transform during the first Seabeam exploration of the EPR was presented by Francheteau *et al.* (1983) and Francheteau and Ballard (1983). Lonsdale (1989a, 1991) used 5 other Seabeam traverses to enhance regional interpretations

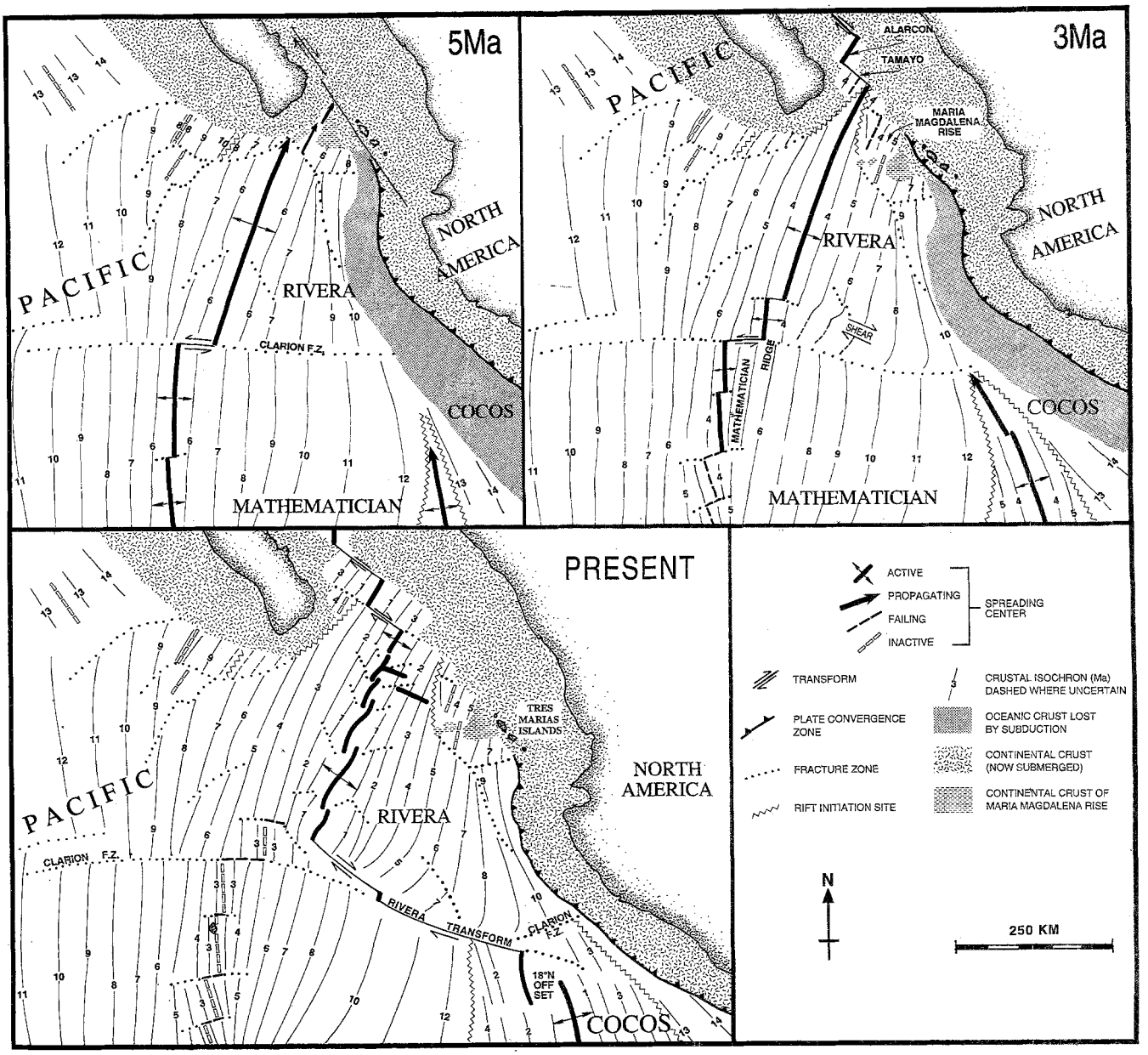

Fig. 1. Tectonic and crustal age patterns around the Gulf of California, at present and at two intervals just before the period discussed in this paper. Patterns are inferred mainly from interpretation of marine magnetic and bathymetric data, revised (with new data) from Lonsdale (1991). Rivera microplate probably split off the Cocos plate along the east-flank Clarion fracture zone as early as 10 Ma, judging from the divergence of Pacific plate crustal isochrons north and south of the fracture zone. Just before 5 Ma a Pacific-Rivera spreading segment propagated into continental crust to separate Maria Magdalena Rise from Baja California, and link up with a shear zone growing between the Pacific and North America plates as Baja California was gradually captured by the Pacific plate. During the next 2 m.y. the initial inter-continental spreading axes were abandoned as they were overlapped by propagation of the main Pacific-Rivera spreading segment. Meanwhile, the southern margin of Rivera microplate was changing as rifting of the Cocos plate gradually transferred lithosphere to the Mathematician microplate. The spreading axis that had lengthened northward along the eastern margin of that microplate reached Clarion fracture zone at about 4 Ma. By this time, even 50 km of former Pacific-Rivera axis immediately north of Clarion transform had acquired the slow east–west spreading diagnostic of Pacific-Mathematician motion. The western part of the Rivera-Mathematician boundary was north of the former Rivera-Cocos boundary along Clarion fracture zone, and at 4–2 Ma a shear zone between the microplates deformed east-flank crust that had accreted to the southern part of the Pacific-Rivera EPR. This shear zone was a precursor of Rivera transform, born when Mathematician microplate was captured by the Pacific plate.

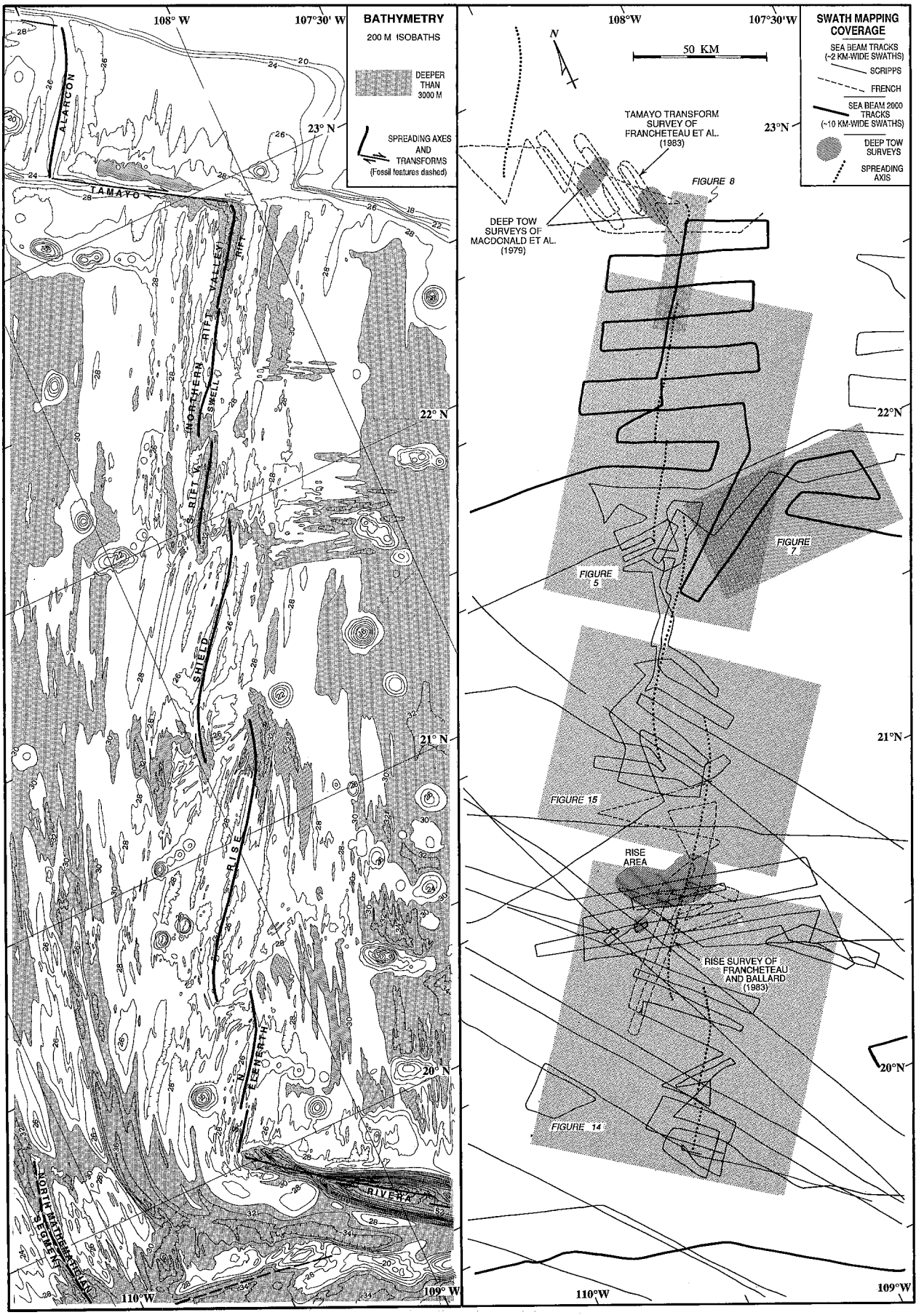
BATHYMETRY
200 M ISOBATHS
DEEPER THAN 3000 M
SPREADING AXES AND TRANSFORMS
(Fossil features dashed)
SWATH MAPPING COVERAGE
SEA BEAM TRACKS (~2 KM-WIDE SWATHS)
SCRIPPS
FRENCH
SEA BEAM 2000 TRACKS (~10 KM-WIDE SWATHS)
DEEP TOW SURVEYS
SPREADING AXIS
108° W
107°30' W
108°W
107°30'W
N
50 KM
23° N
23°N
22° N
22°N
21° N
21°N
20° N
20°N
109° W
109°W
110°W
ALARCON
TAMAYO
TAMAYO TRANSFORM SURVEY OF FRANCHETEAU ET AL. (1983)
FIGURE 8
DEEP TOW SURVEYS OF MACDONALD ET AL. (1979)
FIGURE 7
FIGURE 5
FIGURE 15
RISE AREA
RISE SURVEY OF FRANCHETEAU AND BALLARD (1983)
FIGURE 14
NORTHERN RIFT VALLEY
S RIFT
SHIELD
RISE
CLEMENTE
RIVERA
NORTH RIFT SEGMENT

that were based mainly on conventional sounding lines and to show that small risecrest offsets at 20.5° N and 22.0° N lack transform faults, i.e., are of the nontransform variety.

Methods of this study

This paper interprets previously unpublished observations made with the multibeam sonars on the Scripps Institution's vessels *Thomas Washington* and *Melville.* New bathymetric surveys with ~2 km-wide swaths from a 16-beam Seabeam sonar (Renard and Allenou, 1979) cover non-transform offsets at 22.0° N and 21.3° N, and the axis of the intervening spreading segment. Bathymetry of crust accreted between the 22.0° N offset and Tamayo transform was mapped with ~10 km-wide swaths from a 120-beam Seabeam 2000 system; this sonar also measures the acoustic reflectivity of an equally wide strip of seafloor, and presents the data as a backscatter image on which the rock outcrops of young lava flows and fault scarps are sharply delineated. These surveys have been augmented by several additional Seabeam and Seabeam 2000 transits of the rise (Figure 2).

Multibeam bathymetric and backscatter swaths prove invaluable for establishing the present pattern and strike of spreading axes, and for determining prior patterns that existed during the accretion of crust that is now on the rise flanks. The present EPR spreading axis was identified by the distinctive fine-scale topography (described below) of the volcanically active axial rift zone (neovolcanic zone). In most places this identification was corroborated by recognizing the local magnetic anomaly from an axial magnetization high (Klitgord, 1976). Mapped patterns of "abyssal hill lineations", the boundary scarps of fault blocks comprising the highly lineated terrain of the rise flanks, were assumed to indicate former patterns of the EPR axis. This assumption is based on the observation that these fault scarps develop parallel to the axis on crust less than 0.2 m.y. old (e.g. Francheteau *et al.*, 1981), and are subsequently unmodified except for gradual sediment burial. Lines drawn parallel to abyssal hill lineations therefore approximate crustal isochrons, which can be dated by relating them to the parallel magnetic lineations. In practise, abyssal hill lineations were used to interpolate magnetic stripes between magnetic profiles, and to interpolate crustal isochrons between those defined by magnetic reversals. There are two notable and informative exceptions to the generalization that rise-flank fault scarps are unmodified after leaving the EPR plate boundary zone. Propagation of axial rift zones through preexisting rise flank transfers crust from one flank to the other, with concomitant rotation and strike-slip motion of abyssal hill fault blocks (Searle and Hey, 1983; Kleinrock and Hey, 1989). A second type of rise-flank disruption in the mouth of the Gulf is inferred to result from deformation in a divergent plate boundary zone that intersects the risecrest. Published seismicity data was examined for evidence of these types of off-axis deformation.

As well as mapping and interpreting patterns of fine-scale bathymetry and magnetic anomalies, I employ standard forward-modelling techniques and the Cande and Kent (1992) magnetic timescale to estimate Pacific-North America and Pacific-Rivera spreading rates. The latter, and the mapped pattern of the Pacific-Rivera boundary, allow revised estimates of the relative motion of the Rivera microplate with respect to the surrounding plates.

Objectives of this paper

In addition to improving the estimate of Rivera plate motion and the Pacific-North America spreading rate, this study addresses the following questions, in the course of characterizing the risecrest: (1) *What is the plan pattern of the EPR axis and how has it changed since 2.6 Ma.?* Before the advent of multibeam mapping, many depictions of the plate boundary showed a sinuous axis with no break between Tamayo and Rivera transforms, the supposed sinuosity explaining how the well defined 038° strike of the axis and young magnetic lineations in the RISE area could be so oblique to the overall 025° trend of the rise (see discussion in Macdonald *et al.*, 1980, pp. 3676–3677). However, Larson (1972) inferred from his initial reconnaissance that the axis had been subdivided sometime after 2 Ma by a short lateral offset near 21.3° N, where Sykes (1970) had located strike-slip earthquakes, and after additional offsets at 20.5° N

Fig. 2. Bathymetry of the risecrest, and identification of the spreading segments. Contours are based on multibeam echosounding along the tracks in the right panel, plus conventional echosounding along many more tracks (most of them plotted in the left panel of Figure 3). Shaded rectangles on the multibeam track chart locate more detailed maps presented in subsequent figures.

and 22.0° N had been inferred from other seismicity and magnetic data (Reid *et al.*, 1977; Ness *et al.*, 1981) it became clear that the actual pattern of the axis south of Tamayo transform is a staircase of en echelon spreading segments separated by left steps. This pattern was confirmed by the initial Seabeam traverses (Lonsdale, 1989a). New data presented in this paper complete the description of this staircase and help explain how and why it evolved from a much straighter plate boundary.

(2) *Where is the triple junction that separates axes of Pacific-North America and Pacific-Rivera spreading, and what is the style of deformation on the North America-Rivera boundary?* Atwater (1970) and most subsequent investigators (e.g. de Mets *et al.*, 1987; Ness *et al.*, 1991) placed the triple junction at Tamayo transform, implying that only the Alarcon segment is at the Pacific-North America boundary, and all the segments between Tamayo and Rivera transforms, as well as the east-flank Tamayo fracture zone, bound the Rivera microplate. Larson (1972, Figure 15) inferred that the northern boundary of the microplate (which he mistakenly believed to have been captured by the North American plate at about 2 Ma) was instead near 22° N, 100 km south of Tamayo transform, and coincided with the junction between the new, continent-separating mid-ocean ridge and the remnant of oceanic rise. I present new evidence that at least one segment south of Tamayo transform has Pacific-North America spreading, that the Pacific-North America-Rivera triple junction is of the ridge-ridge-ridge (RRR) type (rather than the ridge-fault-trench junction inferred by de Mets and Stein (1990)), and that North America-Rivera divergence creates broad zones of extensional deformation on the eastern flank of the rise.

(3) *How does the risecrest relief vary from segment to segment and within a single segment?* The cross-section near 21° N at the middle of the best-known segment has been used to typify intermediate-rate (50–90 mm yr^{-1}) spreading centers (Macdonald, 1982), but that was before swath mapping of other medium-spreading rises, notably the Juan de Fuca Ridge (e.g. Karsten *et al.*, 1986; Kappel and Ryan, 1986) emphasized that diversity of risecrest morphology is one of their most striking characteristics (Johnson and Holmes, 1989).

(4) *What is the structure, tectonics and history of nontransform offsets on this slower spreading part of the EPR?* Some of the segment between Tamayo and Rivera transforms resemble nontransform offsets on the fast-spreading EPR (where they are sometimes called overlapping spreading center systems) and on other intermediate-spreading rises (where they are sometimes called propagating rift systems). A convenient result of their nearshore location is more seismicity information, including fault plane solutions, than is available for most mid-ocean examples.

Answers to these questions provide a better regional setting for the detailed studies of spreading center processes that have already been undertaken in the mouth of the Gulf, and a basis for structural comparison with other risecrests. They also bear on such non-provincial problems as the origin of risecrest segmentation, the dynamics of nontransform offsets, the factors controlling risecrest cross-sections, the kinematics of trench-bounded microplates, and the effects of extensionally rupturing young oceanic lithosphere.

I address the four questions in turn, and have found it convenient to discuss the probable answer to each one before presenting the facts relevant to the next, rather than dividing the paper into descriptive and interpretive halves. The questions are interrelated, however, and some of these interrelationships are explored in a final discussion section.

Plan Pattern of the Spreading Axis

Present pattern

Between Rivera and Tamayo transforms the EPR axis is laterally offset a total of 75 km by 6 left steps, those at 20.5° N, 21.3° N and 22.0° N being large nontransform offsets with lateral displacements of 23 km, 27 km, and 14 km. The offsets define 7 spreading segments with an average length of 60 km (Figure 2). Two of these segments, identified as Swell and Rift by Bender *et al.* (1984), share a common axial rift valley. The additional 60 km-long Alarcon spreading segment is isolated from the rest of the system by the 70 km left step of Tamayo transform. Detailed mapping of parts of some segments, e.g., in the RISE area, has revealed several other smaller (< 1 km) left and right steps of the neovolcanic zone (e.g., Ballard *et al.*, 1981). These minor and probably temporary displacements of parts of volcanic rift zones may define a finer scale of segmentation, but require near-bottom observations for verification.

At the larger inter-segment offsets there is extensive overlap of axial rift zones, with inward curvature of the overlapped tips (Figure 2). The straight,

nonoverlapped parts of the axial rift zones between Rivera transform and the 22.0° N offset lie on great circles that converge to the northeast at a nearby point inferred to be the Pacific-Rivera Euler pole. The segment north of the 22.0° N offset diverges from this trend by 7°, and other small but noticeable changes in azimuth of the axis occur in the middle of the Swell segment and at the tiny 22.6° N offset. North of this small left step, spreading axes on both sides of Tamayo transform strike 035 ± 1°, the azimuth of meridians to the far-away Pacific-North America Euler pole of Argus and Gordon (1990).

Prior patterns

Magnetic anomalies and abyssal hill lineations on the young rise flanks (Figure 3) show that the present highly segmented pattern of the spreading axis is of very recent origin, but does have subtle antecedents. The continuity and plan shape of Anomaly 2A.1, unbroken except where perturbed by local seamount anomalies, indicates that only 2.6 m.y. ago there were no lateral offsets between Tamayo transform and the nascent Rivera transform. The observed spatial variation in amplitude of the seamount-free west flank Anomaly 2A.1 (Figure 3) may signify that accretion at this long continuous axis had regular along-strike variations (in crustal thickness or composition) which defined aligned spreading center cells rather than laterally offset segments. Identification of three saddles in this magnetic ridge as "zero offset fracture zones" (Schouten and White, 1980) is encouraged by the observed evolution of the two southern examples into small left-stepping offsets by Chron 2 time (1.98–1.76 Ma).

Another interesting feature of the 2.6 Ma risecrest shown by the pattern of Anomaly 2A.1 is that the unbroken risecrest between Tamayo and Rivera transforms had a 10° bend midway along its length. It thereby resembled the present Gorda Ridge between Blanco and Mendocino transforms (Clague and Holmes, 1987). The Gorda Ridge bend was once inferred to be a triple junction where orthogonally spreading Pacific-Juan de Fuca and Pacific-South Gorda axes met a Juan de Fuca-South Gorda boundary (Riddihough, 1984). Wilson (1989) explained how the obliquity of the southern part of the risecrest to Pacific-Juan de Fuca motion can be explained better by nonrigid behavior of the southern part of the Juan de Fuca microplate, where curving magnetic stripes provide clear evidence for distributed deformation. This explanation probably also applied to the similarly situated southern part of the Rivera microplate, where sharp curvature of east-flank magnetic stripes older than 2.0 Ma indicates severe intra-plate deformation of crust adjacent to the nascent Rivera shear zone (Figure 1).

During Chron 2 the previously unbroken spreading axis had left steps of 3 km and 5 km located 50 km and 150 km north of Rivera transform (Figure 3), ancestors of the 20.5° N and 21.3° N offsets, and another 3 km left step 60 km south of Tamayo transform, ancestral to the short 22.2° N offset (Figure 4). A slight clockwise rotation of the southern half of the spreading axis since Chron 2A had reduced its obliqueness with respect to the northern half to 5°, and the inferred change of spreading direction may have spawned the two southern offsets by the readjustment mechanism of Menard and Atwater (1968). A subsequent 15° clockwise rotation of spreading axes greatly enlarged the displacements of these two left steps, to 85% of their present lengths by Jaramillo time; mapped changes in abyssal hill azimuths date the time of most rapid reorientation as midway between Chron 2 and the Jaramillo event, i.e., about 1.5 Ma. This large Early Pleistocene change in spreading direction affected the risecrest from Rivera transform to 22° N. Magnetic stripes on the rise flanks further north (Figure 4) show much less (~ 3°) clockwise rotation, and the 22.0° N offset developed rapidly after 1.5 Ma as the boundary between a Shield segment that was rotating rapidly clockwise, and a Southern Rift Valley segment that was hardly rotating at all. The small change in spreading direction north of 22° N lengthened the ancestral 22.2° N offset to just 5 km by Jaramillo time, and initiated another small and short-lived left step about 40 km south of Tamayo transform (Figure 4). North of the transform, magnetic anomalies on the seamount-free east flank of the Alarcon segment (Figure 3) record no change in azimuth of the spreading axis between Chron 2 and the Jaramillo event.

The pattern of the risecrest at 1 Ma was very like the present, a staircase of segments separated by left steps of different sizes, with a noticeable change in axial strike at the 22.0° N offset. This "bend" near 22° N was in the opposite direction from the bend of Chrons 2A-2 time. Since the Jaramillo event the plate boundary pattern has changed because of along-axis migration of the nontransform offsets (discussed below), and clockwise rotation of


108° W
107°30' W
50 KM
N
E
W
S
23° N
22° N
21° N
20° N
110° W
109° W
2A
ANOMALY
MAGNETIC PROFILES
SATELLITE NAVIGATED
OTHER
PROFILE OF FIGURE 9
SHEARED CONTL. MARGIN
108°W
107°30'W
ALARCON SMTS.
ALARCON
TAMAYO TRANSFORM
TAMAYO SEAMOUNTS
SWELL
RIFT
RIFT VALLEY)
(NORTHERN
NORTHERN RUPTURE ZONE
22.2° N OFFSET
SOUTHERN RIFT VALLEY
SOUTHERN RUPTURE ZONE
22.0° N OFFSET
SHIELD
21.3° N OFFSET
RISE
RISE AREA
LARSON
GREEN
RED
20.5° N OFFSET
CHANGE IN ABYSSAL HILL AZIMUTH
WEST ELENERTH SMT.
(SOUTH) ELENERTH (NORTH)
RIVERA TRANSFORM
MAGNETIC AXES
CLARION FRACTURE ZONE
AXIAL RIFT ZONE OF EPR (WITH SEGMENT NAME)
ABYSSAL HILL LINEATIONS
TECTONICALLY ROTATED CRUST
SEAMOUNT
SEAMOUNT CHAIN
FRACTURE ZONE
GRANODIORITE/ TONALITE DREDGE
BOUNDARY OF CRUST ACCRETED DURING BRUNHES EPOCH (POST 0·78 Ma)
CRUST ACCRETED DURING JARAMILLO (J) AND OLDUVAI (CHRON 2) EVENTS
PRE - 2·6 Ma OCEANIC CRUST
CONTINENTAL CRUST

spreading axes south of 22.0° N has continued at a very slow rate, presumably recording a correspondingly slow change in spreading direction. During the Brunches epoch a new left step subdivided the Elenerth segment, and a left step that had left a trail near 22.5° N disappeared, or was replaced by the small offset and bend of the axis at 22.6° N.

Identification of Plate Boundaries and Estimates of Plate Motions

The North America-Rivera boundary and the Pacific-North America-Rivera triple junction

One indicator that a plate boundary intersects the EPR crest south of Tamayo transform is the 7° change in risecrest azimuth observed across the short 22.0° N offset. This misalignment is apparent on previous renditions of the risecrest plan (e.g., Figure 2 of de Mets and Stein (1990)), but there has been no discussion of its significance. It could signify a rare instance of oblique EPR spreading along part of a single plate boundary, or the meeting of two different plate boundaries at a risecrest triple junction like those on the equatorial EPR (Lonsdale *et al.,* 1992). Confirmation of a triple junction explanation comes from identifying a change in the along-axis gradient of spreading rate, discussed below, and from mapping a zone of north–south crustal extension with a noneruptive axis that strikes down the eastern rise flank, almost orthogonal to EPR abyssal hills, from near 22° N on the risecrest (Figure 5). Complications to a simple triple junction explanation are the great breadth (50 km) of this zone, and the presence of another east-flank belt of EPR-parallel extension (the 25 km-wide "northern rupture zone" of Figures 2 and 5) midway between 22° N and Tamayo fracture zone.

Fig. 3. Magnetic anomalies map (left panel) mapped by subtraction of the International Geomagnetic Reference Field from magnetometer measurements made along the plotted tracks. Area shown is the same as in Figure 2. Structural interpretation (right panel) is based on the distribution of crustal magnetization inferred from the observed magnetic field, and abyssal hill lineations mapped by multibeam bathymetric and side-scan swaths (only plotted on 0.78–2.6 Ma crust). Seamounts "F", "279", "281" and some of the Larson and Tamayo Seamounts are described by Batiza *et al.* (1984) and Lonsdale and Batiza (1980).

The southern rupture zone is a belt of horst-and-graben faulting which extends east for at least 60 km from Brunhes epoch (post-0.78 Ma) crust of the Southern Rift Valley and Shield segments (Figure 5), across the rise-flank trail of the 22.0° N offset, and into a 30–40 km-wide turbidite plain which separates the EPR from Maria Magdalena Rise (Mammerickx, 1980). Where this broad belt of disruption crosses the EPR flank it has a 10 km-wide axial strip of high relief, with 1 km-wide horsts elevated above the general level of coeval unbroken crust and separated by grabens 300–400 m deep (Figure 6). Fault scarps in this axial strip are slightly sinuous, with an average strike of 295°. The lower scarps in the marginal parts of this belt of faulting have divergent strikes, averaging 300° near the northern margin and 285° near the southern margin. Side-scan images in regions of thinly sedimented young crust (west side of Figure 7) show that rupture zone fault scarps cross-cut preexisting scarps of the abyssal hill fabric without displacing them laterally; the traces of abyssal hill lineations prove that the ridges really are horsts rather than volcanic constructions, while their lack of lateral offset indicates an absence of strike-slip faulting in the rupture zone. On older crust further east the rupture zone scarps become more prominent even as the abyssal hill scarps are obscured by sedimentation. On the western side of the region of turbidite deposition, some grabens in the axial part of the rupture zone form enclosed bathymetric depressions more than 100 m below the general level of the plain, implying that recent downfaulting of the 2.0–2.5 Ma crust there has been even faster than sediment accumulation. There is not enough high-resolution profiler data from the middle of the turbidite plain to examine the growth and demise of faulting within the sediment lens, or to determine whether the basement has been ruptured further east than superficial fault traces have been mapped. At the eastern margin of the plain, the lower slopes of Maria Magdalena Rise have abyssal hill relief with no evidence of past or present disruption by east–west faulting. Near 21°55′ N, 107°55′ W, however, the area of turbidite deposition narrows to an inter-plain gap around the western end of an obstructing seamount chain (Mammerickx, 1980), and grabens near the northern margin of the rupture zone can be traced across the gap and up the western slopes of the seamounts (Figure 7). A deep graben in the axial part of this rupture zone intersects the northwestern end of another 1 km-high seamount chain, built on 2 Ma

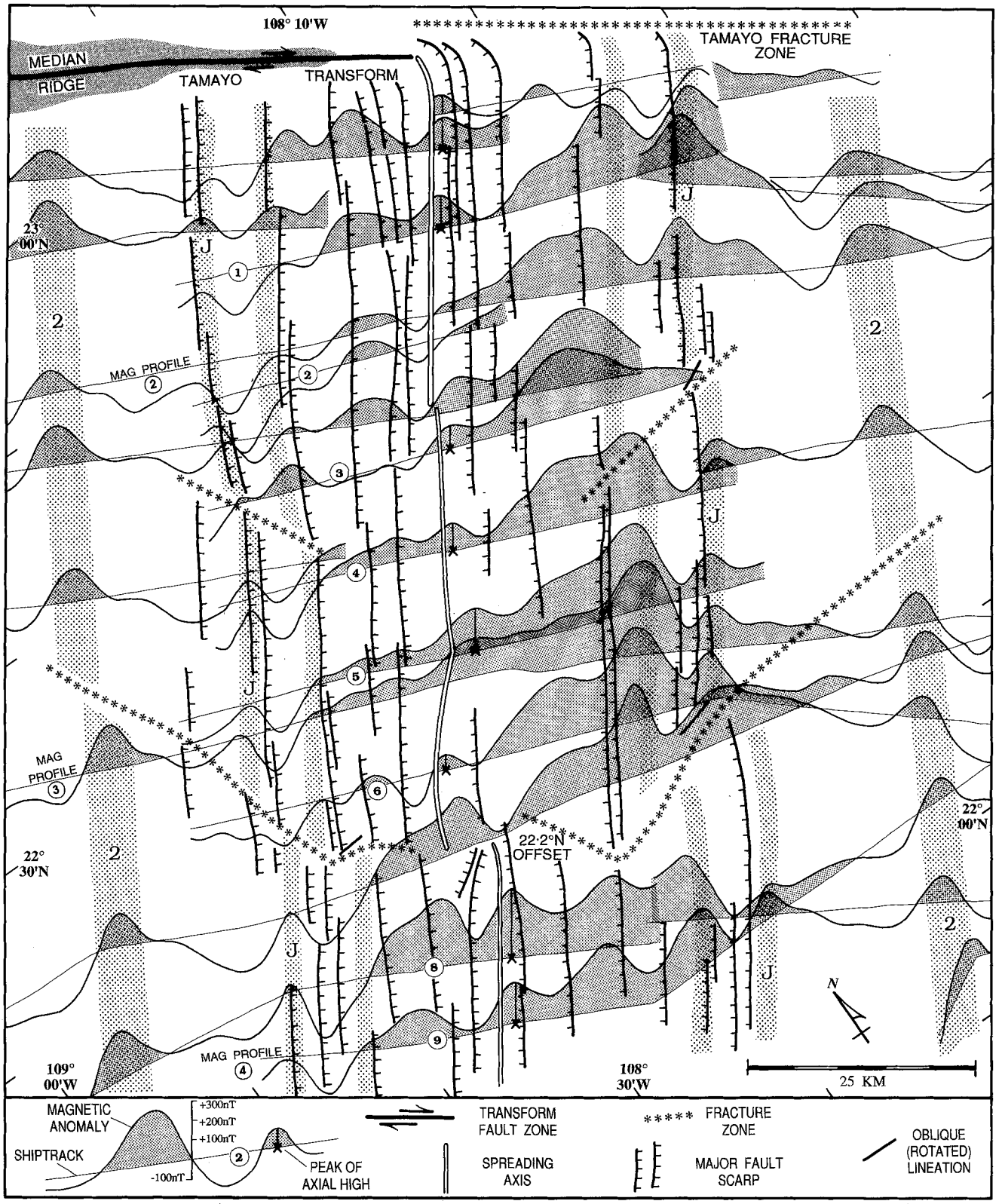

Fig. 4. Magnetic anomalies recorded along satellite-navigated traverses of the risecrest south of Tamayo transform, and the principal rise-parallel fault scarps mapped by a multibeam survey ("east-west" fault scarps of the northern and southern rupture zones are omitted for clarity). Tracks numbered 1–9 were navigated with the Global Positioning System, and have concurrent multibeam bathymetry presented in Figure 12; "mag profiles" 2–4 are also shown, and modeled, in Figure 9. The "oblique fracture zones", traces of small migrating offsets, are inferred from lateral offsets of the anomalies, breaks and curvature of fault scarps, and (in a few places) scarps with the high obliquity typical of tectonic rotation at a nontransform offset.

crust. Fault scarps that continue the graben walls can be traced acros the side-slopes and summits of the coalesced volcanoes (Figure 7), though they have less amplitude there. The pattern and extent of faulting on and around these volcanoes resembles that mapped where seamounts have entered zones of graben formation on the outer slopes of trenches (e.g., Lonsdale, 1986, Pontoise *et al.*, 1986).

The northern rupture zone differs from the southern one in its lack of axial symmetry (Figure 6). A high fault scarp striking 295° along the southern boundary overlooks a down-dropped block which is dissected by a series of 1–2 km-wide grabens that become successively shallower to the north. These grabens have more northerly strikes (300–310°), causing the fault zone to broaden westward toward the EPR crest, and have their greatest bathymetric expression where they cross the thinly sedimented "rift mountain" ridges that characterize this part of the rise flank (Lewis, 1979). On the down-dropped block, the valley between the ridges that follow 0.7 Ma and 1.0 Ma crustal isochrons has a 100–150 m-thick pond of turbidites, sampled further north at Deep Sea Drilling Site 485 (Lewis *et al.*, 1983). Only the southernmost 5 km-wide part of this zone of faulting can be traced across this valley on multibeam bathymetry or side-scan; the shallow northernmost grabens cannot even be traced across a thinner part of the turbidite pond west of the 0.7 Ma ridge. The southernmost belt of intense faulting, with its complex pattern of splaying and scissoring fault scarps (Figure 5) extends eastward at least 5 km beyond the limit of Seabeam 2000 coverage (40 km from the EPR axis) to the 1.76 Ma isochron, where a conventional echosounder traverse shows a 110 m-deep rift valley. Further east, there is no bathymetric or basement-relief evidence of the northern rupture zone on crust older than 2.5 Ma beneath the turbidite plain at the rise margin, which was surveyed with the Seabeam (plus seismic profiler) tracks shown in Figure 2. At the other end of this fault zone, near the EPR crest, grabens cut crust as young as 0.25 Ma. The deep southernmost graben ends in a region of volcanic relief that lacks much superficial evidence of the usual risecrest-parallel faulting and fissuring, though one of the low volcanic shields has a 500 m-diameter pit crater in its summit. Structural lineations displayed on side-scan images, and caused by fissure systems or fault scarps less than 10 m high, prolong the graben-bounding fractures across these evidently young, sediment-free lava flows, to within 3–4 km of the EPR spreading axis at the Swell segment.

The virtual junction of the EPR axis with a principal fracture of the northern rupture zone is the best present approximation to a theoretical "triple point" between the Pacific, North America and Rivera plates. Around this point the risecrest geomorphology changes in two ways that are plausibly related to the unique tectonic situation. First, the Northern Rift Valley that contains this part of the EPR axis is almost filled by a volcanic "swell". Second, near its intersection by the northern rupture zone, the EPR neovolcanic zone swerves away from the mid-line of the axial rift valley so that the triple point is located closed to the rift wall, or more accurately, close to the interpolated position of the rift wall, where it would be but for burial by lava flows (Figure 5). Local bending of the spreading axis toward intersecting axes has been mapped at other RRR junctions on the EPR crest (Lonsdale *et al.*, 1991). The "swerve" of the EPR axis into this triple point from the north is very gradual, distributed throughout the 25 km south of the 22.6° N offset, i.e., along the whole length flanked by the northern rupture zone. South of the triple point, where the east flank of the Northern Rift Valley is intact, the EPR axis bends away from the valley mid-line more sharply. The axis of the southern part of the Swell segment seems to have a strike appropriate for orthogonal Pacific-Rivera spreading (whereas its rift valley walls are normal to Pacific-North America motion), but the straight section is so short, before curving into the 22.2° N offset (Figure 5), that precise measurement of its azimuth is difficult. The next segment to the south, the Southern Rift Valley, definitely does not lie on a Pacific-Rivera meridian. Instead, its axis, rift valley walls, and rise flank lineations on post-1 Ma crust, have 032° ± 2° strikes more northerly even than Pacific-North America meridians. They are parallel to the axis of the northern part of the Swell segment, the part flanked by the northern rupture zone. The Southern Rift Valley segment is flanked by the southern rupture zone. At both sites of deviant strikes, the EPR axis separates, or has separated, the Pacific plate from broad east-flank deformation zones, rather than from intact plates.

I interpret the fault scarps of the two rupture zones as superficial expressions of recent and continuing extensional rupture of the young EPR lithosphere which spreads east from the risecrest; lithosphere which spreads west as part of the Pa-

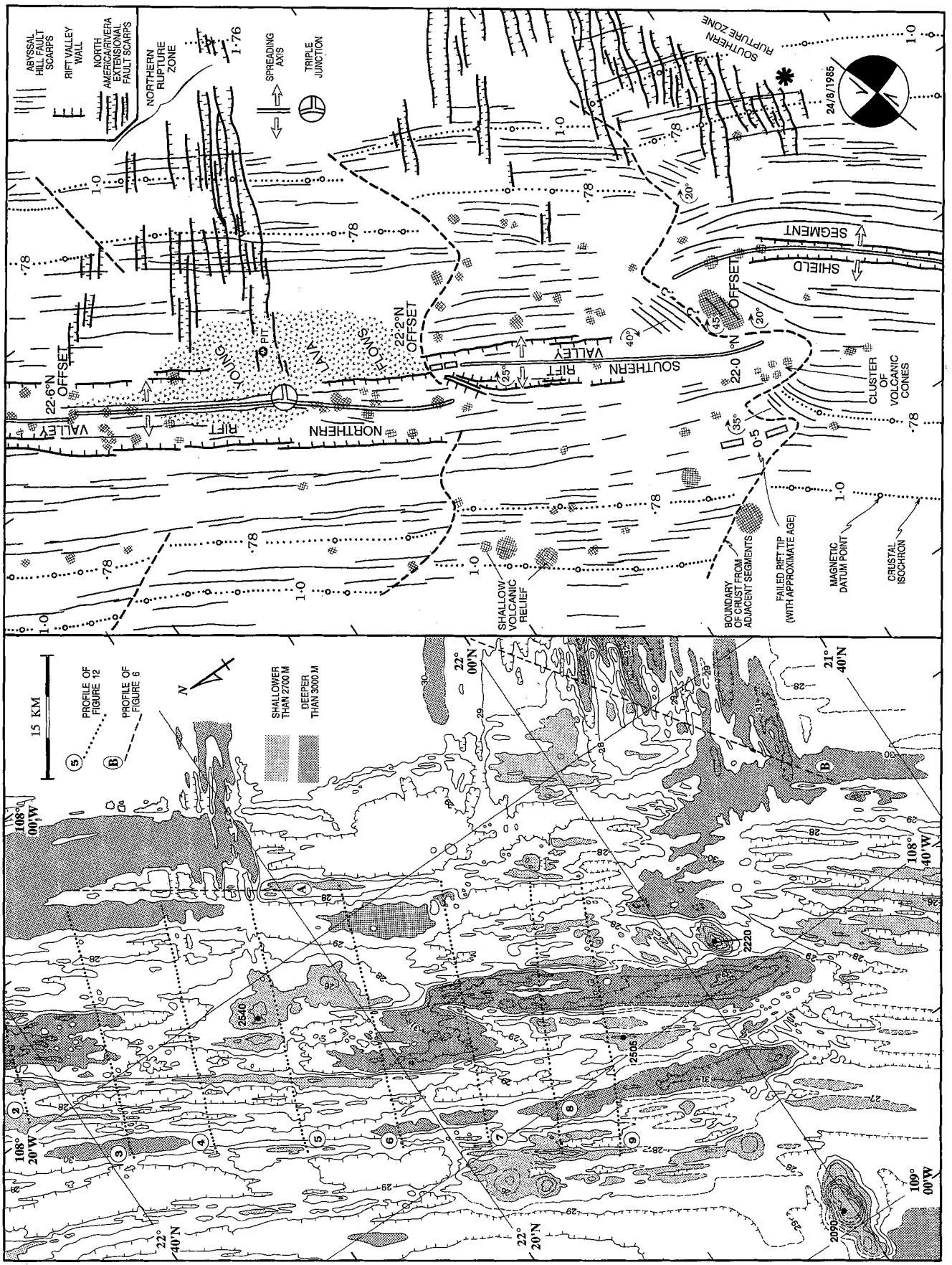
ABYSSAL HILL FAULT SCARPS
RIFT VALLEY WALL
NORTH AMERICA/RIVERA EXTENSIONAL FAULT SCARPS
NORTHERN RUPTURE ZONE
SPREADING AXIS
TRIPLE JUNCTION
SOUTHERN RUPTURE ZONE
24/8/1985
SEGMENT
SHIELD
OFFSET
22·6°N OFFSET
22·2°N OFFSET
NORTHERN RIFT VALLEY
SOUTHERN RIFT VALLEY
PIT
CLUSTER OF VOLCANIC CONES
SHALLOW VOLCANIC RELIEF
BOUNDARY OF CRUST FROM ADJACENT SEGMENTS
FAILED RIFT TIP (WITH APPROXIMATE AGE)
MAGNETIC DATUM POINT
CRUSTAL ISOCHRON
15 KM
PROFILE OF FIGURE 12
PROFILE OF FIGURE 6
SHALLOWER THAN 2700 M
DEEPER THAN 3000 M
108° 00'W
108° 20'W
108° 40'W
109° 00'W
22° 00'N
22° 20'N
22° 40'N
21° 40'N
2540
2506
2220
2090

cific plate is not affected. The lithosphere-breaking tensional stress in the east flank is probably oriented normal to the 295° strike of the principal fault scarps, i.e., within 10–15° of parallel to the risecrest. The asymmetry and westward fanning of the northern rupture zone may signify that the principal failure surface there is a north-dipping detachment which outcrops along the southern margin of the zone, underlies the fractured down-dropped block, and shoals as the lithosphere thins westwards (Figure 6). The observed fault pattern of the southern rupture zone requires that if lithospheric failure was by detachment faulting, then the detachments in this zone dip both north and south from the high-relief axial strip. An alternative explanation for the eastward convergence of fault scarps in both rupture zones is that all the superficial fractures are aligned with axes of regional tensional stress which converge at two nearby Euler poles. This alternative is discounted because it implies an implausibly simple style of lithosphere failure but an unnecessarily complex pattern of plates, and because it does not account for the cross-sectional relief. Nevertheless, locating the North America-Rivera Euler pole, toward which the rate of plate separation decreases to zero, near the east end of the rupture zones would explain their abrupt eastern termination, and the absence of any significant eastward increase in the amount of crustal extension across the rupture zones, even though the crust ages in that direction and is therefore likely to have been extended for a longer period of time. Nowhere has crustal rifting developed into crust-accreting North America-Rivera spreading. The amount of horizontal extension in a transect of each zone can be estimated (very approximately) by summing the heights of all east–west fault scarps on the Figure 7 traverses, and assuming dips of 60° for the near-surface faults; this method yields estimates of 1 km of extension in the northern zone and 2 km in the southern zone.

From the previously discussed evidence of rise-flank bathymetric and magnetic lineations, I infer that the triple junction between non-parallel Pacific-North America and Pacific-Rivera segments shifted south to the 22° N area (probably from Tamayo transform) at 1.5 Ma, giving birth to a new North America-Rivera boundary, the southern rupture zone. This plate boundary zone extensionally ruptured pre-1.5 Ma rise-flank lithosphere, including two young seamount chains, as far east as the vicinity of the North America-Rivera Euler pole. The shift of the triple junction coincided with the change in Rivera plate motion that caused a 15° clockwise rotation of Pacific-Rivera spreading segments. Conversion of the EPR axis between Tamayo transform and the new 22° N triple junction from a Pacific-Rivera boundary to a Pacific-North America boundary also caused a clockwise rotation of spreading, albeit of only 3°. This implies that before 1.5 Ma, Pacific-Rivera and Pacific-North America vectors had been very similar in this region, and that the slow relative motion on any North America-Rivera boundary which intersected the EPR almost orthogonally (e.g., the east flank Tamayo fracture zone) had been compressional rather than extensional.

After its birth, the southern rupture zone acted as the slowest spreading limb of an RRR triple junction, lengthening westward while EPR spreading proceeded. I infer that the triple junction subsequently shifted 50 km northward to its present location, giving birth to the northern rupture zone; the partly overlapped southern rupture zone continued as an active plate boundary, but did not continue to lengthen into zero-age EPR crust. Constraints on the timing of this second shift are poor. Coincident readjustment of EPR spreading axes may have eliminated the left step of the risecrest near 22.5° N, which has left no perceptible trail on crust younger than 0.7 Ma. Excessive volcanism at the west end of the northern rupture zone has piled lava on lithosphere with an interpolated age of 0.5 Ma. Lack of parallelism between the rift valley walls and the neovolcanic zone south of the new junction could be evidence that the shift has occurred only in the past 0.1–0.2 m.y., consistent with the immaturely asymmetric structure of the northern rupture zone.

The opening rate of this pair of extensional North America-Rivera segments starts out slow,

Fig. 5. The EPR crest around the 22.0° N, 22.2° N and 22.6° N offsets and the western ends of the northern and southern rupture zones. Bathymetry at 100 m contour interval, in left panel, is mainly from multibeam surveys (see Figure 2 for track coverage) with broken contours interpolated using conventional soundings. Crustal structure and age (right panel) is inferred from bathymetric and magnetic data. Numbers (degrees) enclosed by curving arrows indicate amount and direction of tectonic rotation of adjacent crust. The asterisk is where the U.S. Geological Survey located a 24/8/1985 earthquake that was probably caused by left-lateral strike-slip faulting, as shown by the representation of the centroid moment tensor solution (Dziewonski *et al.*, 1986); a geologically more plausible location of this earthquake is 25 km away in the deforming crust within the 22.0° N offset.

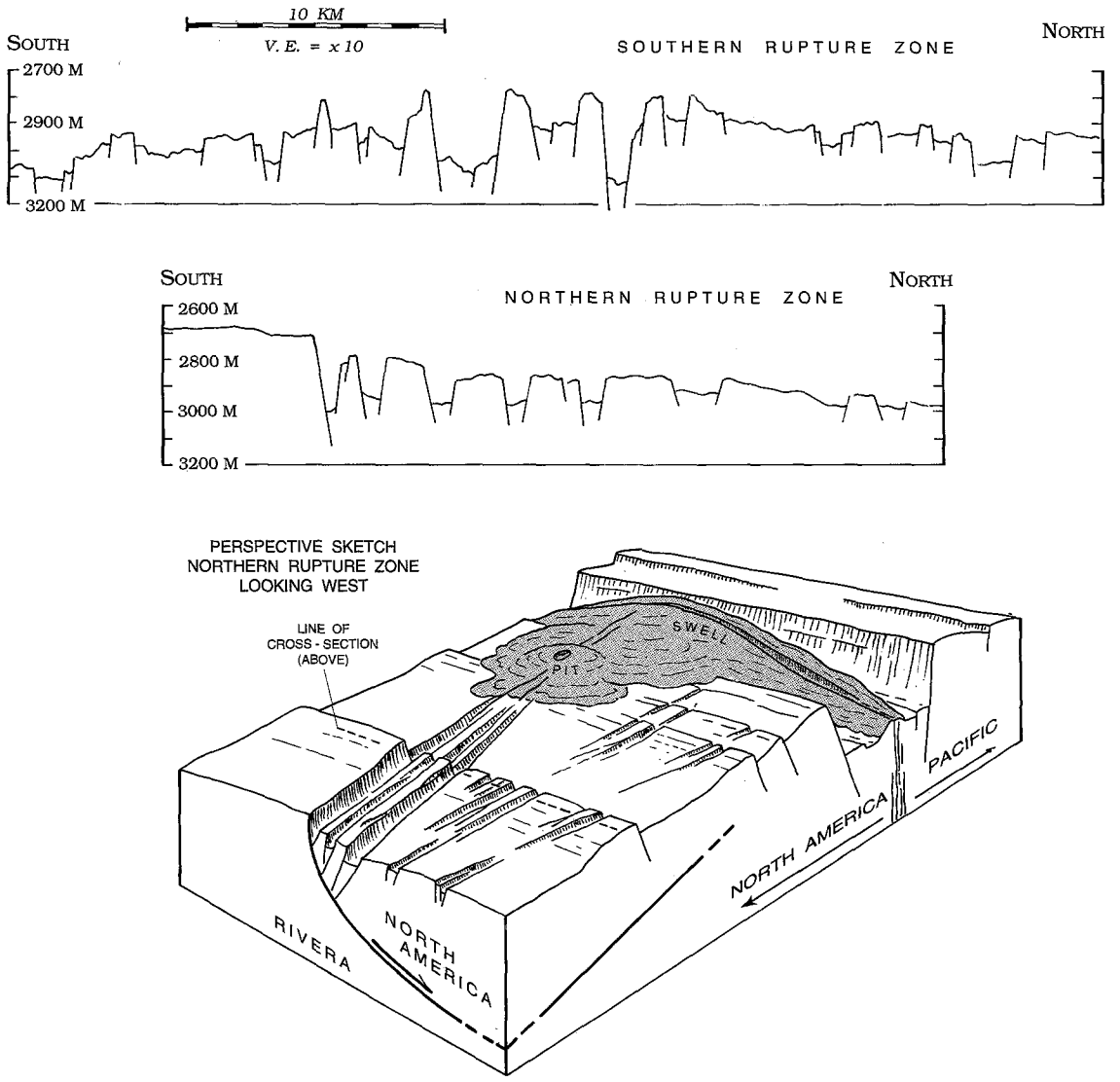

Fig. 6. Bathymetric traverses projected parallel to the risecrest (i.e. at 035°) across the northern and southern rupture zones on the east flank on the EPR, located on the left panel of Figure 5. Fault locations inferred from multibeam bathymetric and side-scan data. Profile B is the center-beam profile of a Seabeam 2000 swath; profile A has been constructed from several adjacent Seabeam 2000 swaths. The block diagram shows the principal fractures of the northern rupture zone extending through a pit crater to the summit of a rifted volcanic swell which almost fills this part of the Northern Rift Valley, and suggests that the asymmetry of this rupture zone could result from faulting above a northward dipping detachment between Rivera and North America lithosphere.

and decreases as the crust spreads east toward the North America-Rivera pole. Even though the southern zone has been active for more than 1 m.y., it has not evolved into a North American-Rivera spreading axis, nor even into a major rift valley like those found in advance of spreading at some other triple junctions, e.g. Hess Deep (Lonsdale, 1988) and SWIR Valley Deep (Mitchell, 1991). Low strain rates may also explain why these parts of the North America-Rivera boundary, and the left-lateral shear zone that presumably connects them, are so poorly delineated by teleseismically recorded earthquakes.

Pacific-North America boundary

The Alarcon spreading segment has been part of the Pacific-North America boundary since it evolved from an intercontinental rift valley and began accreting oceanic crust at about 3.6 Ma (Lonsdale, 1989). An earlier spreading center on Maria Magdalena Rise had this role for the preceding 1.5 m.y.,

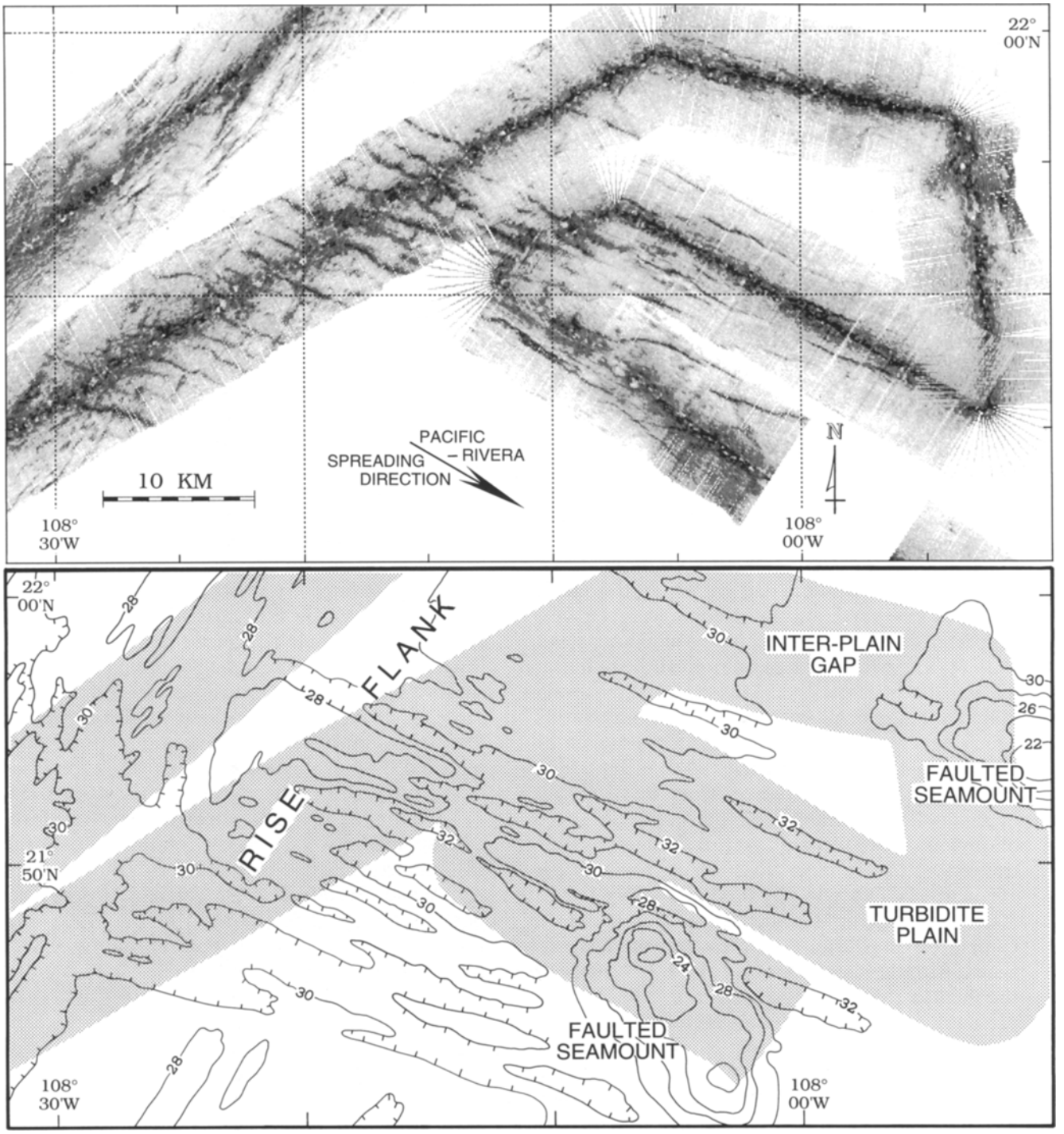

Fig. 7. A patch of the east flank and margin of the EPR (located in Figure 2) that is broken by the southern rupture zone, an extensional part of the Rivera-North America boundary. Upper panel presents Seabeam 2000 data delineating young horsts and grabens which cross northeast-striking abyssal hills (in the west) and a seamount-studded turbidite plain in the east. Lower panel shows bathymetry of the same area, at a 200 m contour interval; shading identifies the extent of sidescan coverage.

but it was overlapped by a new northward-propagating segment of the Pacific-Rivera EPR and abandoned at about 3 Ma (Figure 1). Then, as described above, a 120 km southward shift of the Pacific-North America-Rivera triple junction at 1.5 Ma reestablished Pacific-North America spreading south of Tamayo transform, though a recent 50 km northward shift of the junction has shortened this axis to now include just the Rift segment and the northern half of the Swell segment.

Tamayo transform has also been part of the Pacific-North America boundary throughout the opening of the Gulf of California. Submersible studies (Choukroune *et al.,* 1981; Gallo *et al.,* 1984) have located the present trace of the strike-slip fault zone along the northern side of a shallow transform valley which strikes 305° from the eastern risecrest intersection. Location of the plate boundary zone is less obvious in the western half of the transform, where there is a 500–800 m-high median ridge (Kastens *et al.,* 1979) veneered with mud and rubble (Choukroune *et al.,* 1981). The suggestion of Macdonald *et al.* (1979) and Choukroune *et al.* (1981) that the western part of the fault zone is offset 10 km north of the median ridge is not supported by the Seabeam survey of Francheteau *et al.* (1983), which mapped uninterrupted abyssal hill lineations across the supposed location of the fault zone. Analogy with other EPR transforms which have rubble-strewn median ridges, such as Clipperton transform (Kastens *et al.,* 1986), suggests that the median ridge contains the strike-slip boundary and is a transpressive structure. Absence of obvious strike-slip fault traces on a submersible traverse of the Tamayo ridge (Choukroune *et al.,* 1981) can be explained by the lower slip rate and faster hemipelagic sedimentation, compared to Clipperton transform. Transpression would be consistent with the slight obliquity of the 300° strike of the median ridge (Francheteau *et al.,* 1983) to the present Pacific-North America vector, and has been a common response of right-lateral shear zones along this plate boundary to minor Plio-Pleistocene rotation of the relative plate motion (e.g. Crouch *et al.,* 1984).

Evidence that the Rift segment is on the Pacific-North America boundary, and has been since before the Jaramillo event, includes (1) the parallelism of the Northern Rift Valley to the axis of Alarcon Rise and to a great circle to the Pacific-North America Euler pole; (2) the orthogonal intersection mapped (Figure 8) between the Rift segment and Tamayo transform; and (3) a uniformity in post-Jaramillo spreading rates north and south of Tamayo transform.

The record of crustal accretion at the Alarcon segment has been recognized as a valuable geologic monitor of Pacific-North America motion, but there has been disagreement about how to read this record (Ness *et al.,* 1991). Large seamounts that cover much of the west flank within 50 km of the axis (Figure 3) produce nonlineated magnetic anomalies which hamper magnetic dating of basement, except in narrow seamount-free strips along the northern and southern margins of this segment. The *Thompson* 1975 traverse along the southern margin (Lewis *et al.,* 1983) was not considered by de Mets *et al.* (1987) or Ness *et al.* (1991), and is presented as profile 1 of Figure 9. It is best fit with a Pacific-North America spreading rate that accelerates from 48 mm yr^{-1} to 52 mm yr^{-1}, consistent with de Mets *et al.*'s (1987) interpretation of other, noisier, profiles.

Other *Thompson* 1975 profiles across the Rift and Swell segments south of Tamayo transform (profiles 2 and 3 of Figure 9) also record 52 mm yr^{-1} of accretion since the Jaramillo event, with symmetric spreading on the Rift segment and slight asymmetry, favoring the North American plate and eliminating a 4 km left offset, on the Swell segment. Magnetic profile 4, across the Southern Rift Valley, shows a slightly higher spreading rate, and a similar sense of asymmetry. All these modeled profiles have only Transit satellite navigation, but they are matched by more recent GPS-navigated traverses of Jaramillo and younger crust (Figure 4).

Spreading at 52 mm yr^{-1} near Tamayo transform corresponds to a 0.81° $m.y.^{-1}$ rotation around the instantaneous Pacific-North America Euler pole of Argus and Gordon (1990), which is close to the post-3 Ma stage pole (de Mets *et al.,* 1990). The geodetically determined rotation rate is 0.806° $m.y.^{-1}$ (Argus and Gordon, 1990).

Pacific-Rivera boundary

The Shield, Rise, and Elenerth segments have been part of the Pacific-Rivera boundary since their inception. Other components are the Rivera transform system, which includes several short mid-transform spreading axes, and probably the EPR segment that orthogonally intersects the east end of the transform at 18°30′ N, 106°15′ W (Bourgois *et al.,* 1988), and is separated from the northernmost Pacific-Cocos segment by a large nontransform offset at 18° N.

Since the 1.5 Ma change in spreading direction there has been a steep along-axis gradient in the

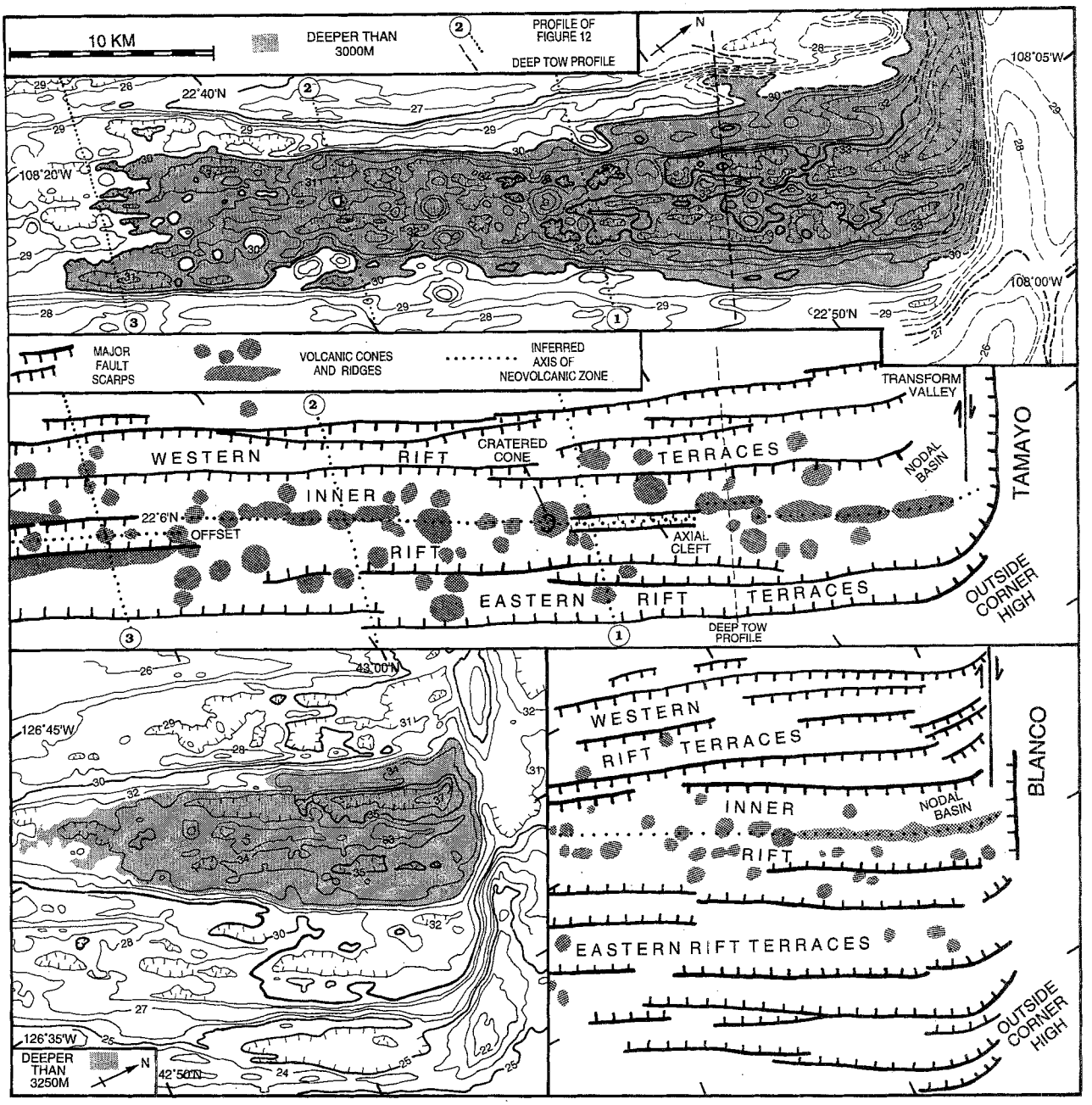

Fig. 8. Bathymetry and interpreted structures of the intersection of the EPR Northern Rift Valley and Tamayo transform (upper panels), compared to the Gorda Rift Valley/Blanco transform intersection (bathymetry from Malahoff, 1984). The maps are all to the same scale, but the contour interval is 50 m for the EPR (top panel), 100 m for Gorda Ridge (lower left).

rate of Pacific-Rivera spreading, in contrast to the almost uniform rate along the Pacific-North America EPR, which is far from its Euler pole. The 54 km of crust accreted since 1 Ma at the Shield segment (profile 5, Figure 9) is only slightly more than on the southernmost Pacific-North America segment; the 66 mm yr^{-1} rate during this time at the Elenerth segment, 170 km to the south (profile 7, Figure 9), is only slightly less than on the Pacific-Cocos axis south of 18° N. The Early Pleistocene adjustment in spreading direction followed the model of segment creation and rotation proposed by Menard and Atwater (1968) rather than the propagating rift model of Hey *et al.* (1988), so there were large and laterally variable asymmetries in crustal accretion between Chron 2 and the Jaramillo event, making it difficult to determine spreading rates during this interval from magnetic profiles that do

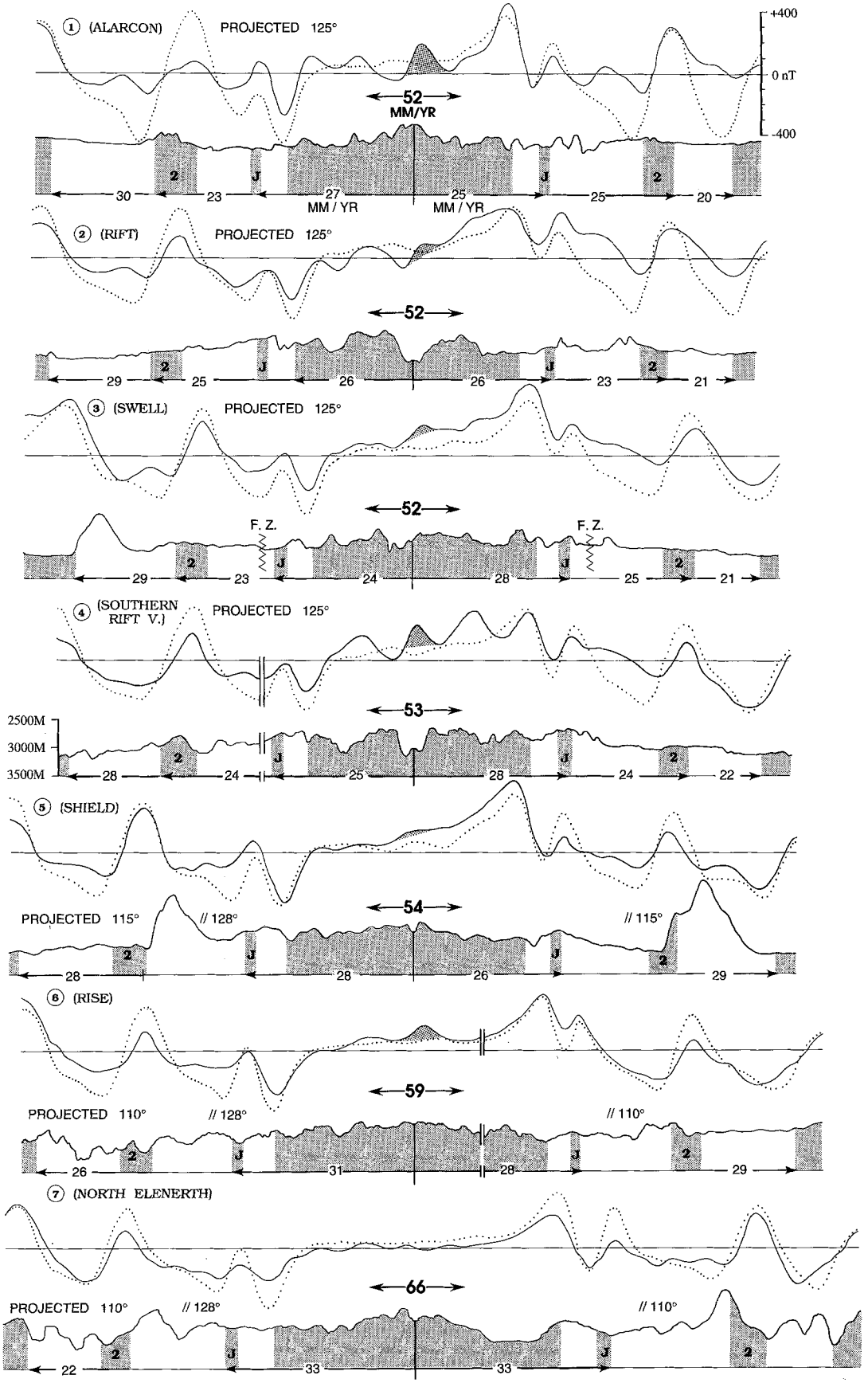
① (ALARCON)
PROJECTED 125°
+400
0 nT
-400
52
MM/YR
30
23
27
MM / YR
25
MM / YR
25
20
② (RIFT)
PROJECTED 125°
52
29
25
26
26
23
21
③ (SWELL)
PROJECTED 125°
52
F. Z.
F. Z.
29
23
24
28
25
21
④ (SOUTHERN RIFT V.)
PROJECTED 125°
53
2500M
3000M
3500M
28
24
25
28
24
22
⑤ (SHIELD)
PROJECTED 115°
// 128°
54
// 115°
28
28
26
29
⑥ (RISE)
59
PROJECTED 110°
// 128°
// 110°
26
31
28
29
⑦ (NORTH ELENERTH)
66
PROJECTED 110°
// 128°
// 110°
22
33
33

not follow the sinuous flowlines. It is clear that before 1.5 Ma, when the Rivera plate extended further north, Pacific-Rivera spreading was slower, and the along-axis gradient in rates was less (Lonsdale, 1989; de Mets and Stein, 1990). The change at 1.5 Ma can be described as a southward shift of the Pacific-Rivera Euler pole, and an acceleration of the plate rotation around it.

de Mets and Stein (1990) describe the Pacific-Rivera vector for the Brunhes epoch as a rotation of 3.986° m.y.$^{-1}$ around a pole at 27.9° N, 103.8° W, but admit that this estimate gives a poor fit to the mapped azimuth of the western part of Rivera transform, and to the focal mechanisms of earthquakes there. The strikes of Rivera transform fault zones are well defined by multibeam bathymetry, and are consistent with the published focal mechanisms. I have chosen to locate the present Pacific-Rivera pole bathymetrically, by assuming that Pacific-Rivera spreading axes (outside of the Rivera transform system) lie on meridians to it, and that the fault zones of the Rivera transform system follow small circles around it (Figure 10). My estimate is that the present pole is at 26.4° N, 104.3° W, only 600 km north of the Pacific-North America-Rivera triple junction. The best estimator of the present rotation rate is the width of the central anomaly along the Pacific-Rivera EPR, despite the evidence from rise flank lineations that the Euler vector continued to shift slightly during the Brunhes epoch (the probable reason that my estimate of the present pole differs from that of de Mets and Stein (1990)). The width of the central anomaly on profiles 5–7 of Figure 9, on 3 other GPS-navigated traverses, and Figure 6 of de Mets and Stein (1990), is best fit with a rotation rate of 4.65° m.y.$^{-1}$ around the 26.4° N, 104.3° W pole.

Fig. 9. Observed (solid line) and synthetic (dotted line) magnetic profiles across segments of the Pacific-North America and Pacific-Rivera EPR, located in Figure 3. Magnetic and accompanying bathymetric profiles (the latter at 10× vertical exaggeration) have been projected approximately normal to magnetic lineations. Magnetic modelling assumed a 1 km-thick layer of 7 a/m magnetization; no attempt was made to model the axial magnetic high (shaded) inferred to be caused by more highly magnetised fresh rock. Bold numbers between diverging arrows are estimated post-Jaramillo spreading rates; smaller numbers below each bathymetric profile are estimated rates of accretion to each flank for the strips between head and tail of the arrows. "FZ" indicates crossing of an oblique, small-offset fracture zone. Source of each profile is: 1–3) *Thompson* Cruise 99, 1975; 4) Scripps Expedition PLUTO, 1982 and RAITT, 1988; 5) Scripps Expedition IGUANA, 1972; 6) Scripps Expeditions COCOTOW, 1974 and CERES, 1982; and 7) Scripps Expedition DEEPSONDE, 1975.

Motion of Rivera microplate

Adding the Euler vector calculated for present Rivera-Pacific motion (4.65° m.y.$^{-1}$ around 26.4° N, 104.3° W) to published vectors for present motion of the Pacific plate with respect to the hotspot reference frame (Gripp and Gordon, 1990), the North America plate (Argus and Gordon, 1990) and the Cocos plate (Macdonald *et al.*, 1992) yields the following results:

1. Absolute motion of the Rivera microplate is estimated to be 3.9° m.y.$^{-1}$ counter-clockwise around 18.4° N, 106.1° W. This location of this pole of no motion, near the east end of Rivera transform (Figure 10B), explains why the 102° strike of the eastern end of this fault zone (Bourgois *et al.*, 1988) is parallel to absolute Pacific motion.
2. Rivera-North America motion is estimated to be 4.0° m.y.$^{-1}$ around a pole at 21.8° N, 107.8° W, on the Rivera-North America boundary at the east end of the southern rupture zone (Figure 10B). This pole location is consistent with the aximuth and abrupt eastern termination of the southern rupture zone, though not with the azimuth of the parallel master fracture of the northern rupture zone. The maximum extension rate predicted at the west end of the southern rupture zone is only 4 mm yr^{-1}. East of the Euler pole, the microplate is converging with North America, causing uplift of Maria Magdalena Rise and slow underthrusting along the almost aseismic northwestern end of the Middle America Trench. The maximum convergence rate is estimated to be 31 mm yr^{-1} at the southeastern end of this plate boundary, where North America overrides stagnant oceanic lithosphere near the absolute rotation pole of the microplate.
3. Rivera-Cocos motion is estimated to be 2.8° m.y.$^{-1}$ around a pole at 17.6° N, 101.1° W, well east of the short boundary zone between these plates. This vector is consistent with fault plane solutions for strike-slip earthquakes in this boundary zone. It predicts 20 mm yr^{-1} of left-lateral slip along 012° at the site of the best constrained solution, a left-lateral slip on a plane striking between 005° and 015° (Eissler and McNally, 1984). This motion is also almost equivalent to the absolute motion of Cocos lithosphere past the stationary corner of the microplate.

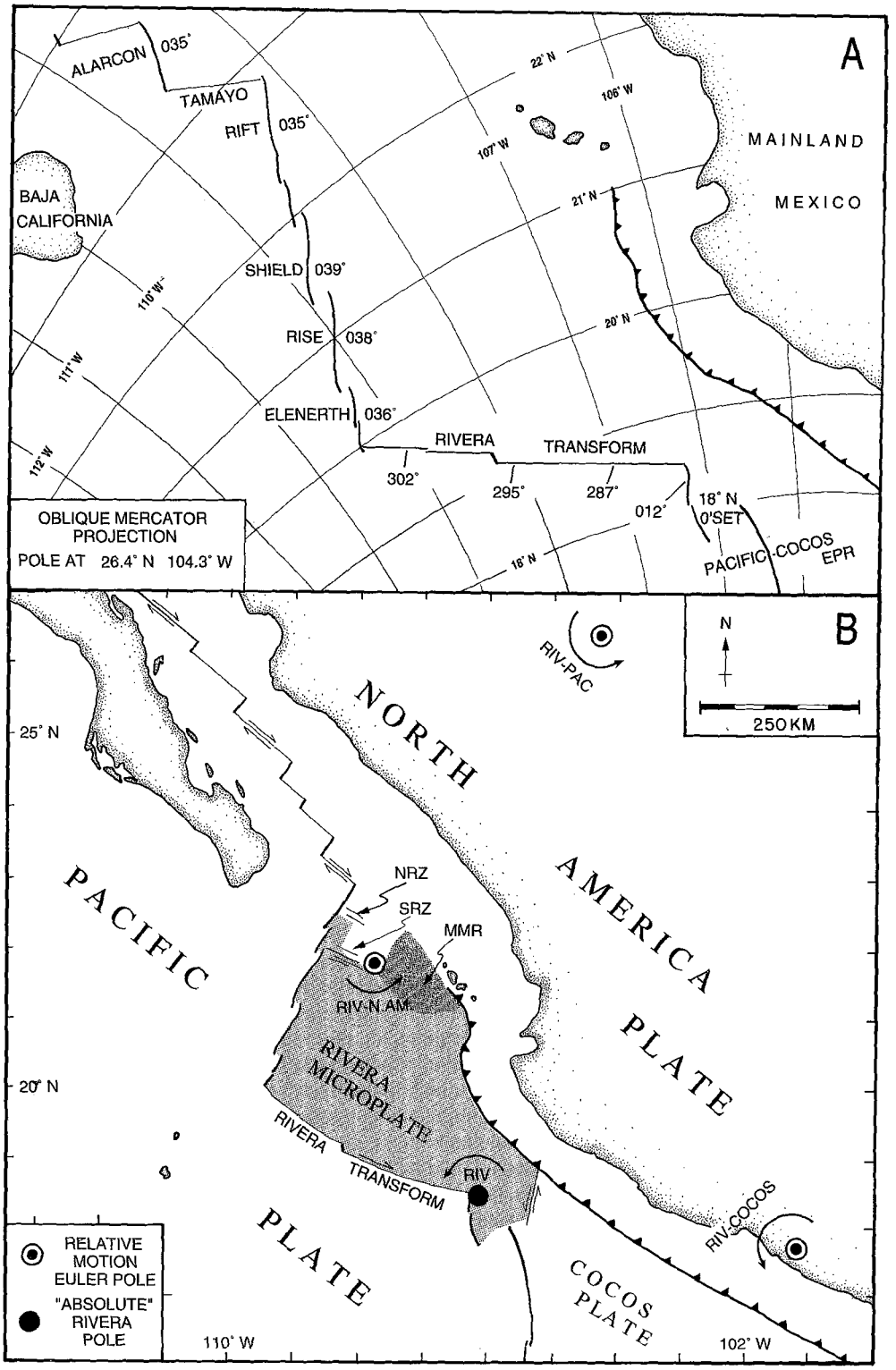

Fig. 10A. The mouth of the Gulf of California on a projection in which meridians to the 26.4° N 104.3° W Pacific-Rivera Euler pole are straight vertical lines (e.g., the axes of the Shield, Rise and Elenerth segments), and small circles around the pole plot as straight horizontal lines (e.g., Rivera transform). Numbers in degrees are the observed strikes of plate boundary zones, as mapped by multibeam surveys. Note that the 012° strike of the spreading axis between Rivera transform and the 18° N nontransform offset is consistent with orthogonal Pacific-Rivera spreading, unlike the 035° strikes of the Alarcon and Rift axes (inferred to be on the Pacific-North America boundary).

B. Estimated Rivera microplate Euler poles. NRZ and SRZ are the northern and southern rupture zones; MMR is Maria Magdalena Rise, an area of shallow 8–3 Ma oceanic crust plus some continental fragments (Figure 1).

The motion of major oceanic plates is primarily determined by the slab pull force toward their marginal trenches, but studies of some EPR microplates (albeit, ones lacking subducting margins) indicate that their motion is caused by the drags of the surrounding major plates (Schouten *et al.*, 1993; Larson *et al.*, 1992). The absolute motion of the Rivera microplate is everywhere obliquely away from its trench, so it seems unlikely that slab pull, by the ~ 10 Ma lithosphere that is being overridden, dominates its motion. Diagnostic features of edge-driven microplates are relative-motion poles located on the microplate boundary, dividing that boundary into convergent and extensional zones. The Rivera-North America pole fits this description, being partway along the new risecrest-to-trench boundary initiated at 1.5 Ma when the northern part of the microplate was captured by the North America plate. The locations of the other relative motion poles indicate that the microplate is not spun by the motion of the Pacific and Cocos plates, perhaps because their divergent drags along the southern boundary cancel each other out. If the Rivera-Cocos pole were on the short southeast boundary of the microplate, then near the Rivera-Cocos-North America triple junction at the Middle America Trench the rates of underthrusting of Rivera and Cocos plates would be similar, whereas the abrupt change in trench seismicity at the junction (Eissler and McNally, 1984) suggests that they are very different.

In the first part of the post-2.6 Ma period the Rivera microplate may have been driven principally by shear stress on its southern boundary. This boundary evolved rapidly between 5 Ma and 1.5 Ma, as lithosphere on its south side belonged successively to the northeast-moving Cocos plate, the clockwise-rotating Mathematician microplate, and eventually the northwest-moving Pacific plate (Figure 1). During Chrons 2A and 2, when the southern boundary was a broad right-lateral shear zone between the Rivera microplate and lithosphere that was acquiring Pacific motion as spreading slowed to a halt on the northern Mathematician Ridge, the westward drag that internally deformed the southern part of the microplate probably drove the Rivera plate westward and slowed Pacific-Rivera spreading. I propose that establishment of Rivera transform, leading to reduction of microplate-rotating stress transmitted across the southern boundary, was the immediate cause of the 1.5 Ma change in Rivera plate motion, with its accompanying acceleration and segmentation-inducing rotation of the Pacific-Rivera spreading center, and initiation of a new diffuse Rivera-North America boundary. If so, the indirect cause was the slightly earlier complete capture of Mathematician microplate by the Pacific plate.

Geomorphology of EPR Spreading Segments

Overall relief, and terminology

Most multibeam traverses of the risecrest show 50–100 m of local relief in the 1 km-wide axial band that probably corresponds approximately to the neovolcanic zone of active fissure eruption and dike intrusion (Ballard *et al.*, 1981; Macdonald *et al.*, 1983). The long profile of this axial band (Figure 11) has broad summits near the middle of each spreading segment, from which the rift zones plunge 200–700 m to their tips. An exception is the Rift segment, where a steady deepening of the axis toward the Tamayo transform intersection continues the northward plunge of the Swell segment away from its summit at the Pacific-North America-Rivera junction. The neovolcanic zone is the shallowest part of this risecrest only along short lengths of the Rise segment, and probably parts of the Alarcon segment; elsewhere it occupies an axial depression overlooked by the crests of off-axis fault scarps (Figure 11).

Describing risecrest depressions and elevations involves using terms freighted with genetic connotations. The terms I use, and now define, imply structural interpretations which are discussed later. Axial rift valleys, also known as median valleys, are large scale structures characteristic of slow-spreading ridges, where they are typically 20–30 km wide and 1000–2500 m deep, but examples near the smaller end of this range occur on some Pacific rises with medium spreading rates (e.g., Clague and Holmes, 1987). They are maintained by uplift into the marginal rift mountains of slivers of crust that accreted on the rift valley floor, as demonstrated by the presence of sediments diagnostic of the rift floor on steps (rift terraces) forming the rift walls (Atwater and Mudie, 1973). Another smaller variety of axial rift valley, only 4–10 km wide and 100–250 m deep, and perhaps corresponding just to the "inner rift" of the larger variety, is more typical of intermediate spreading (e.g. Lonsdale, 1977b; van Andel and Ballard, 1979). The mid-lines of both size classes of axial rift valleys typically have small volcanic constructions, elongate ridges and partly

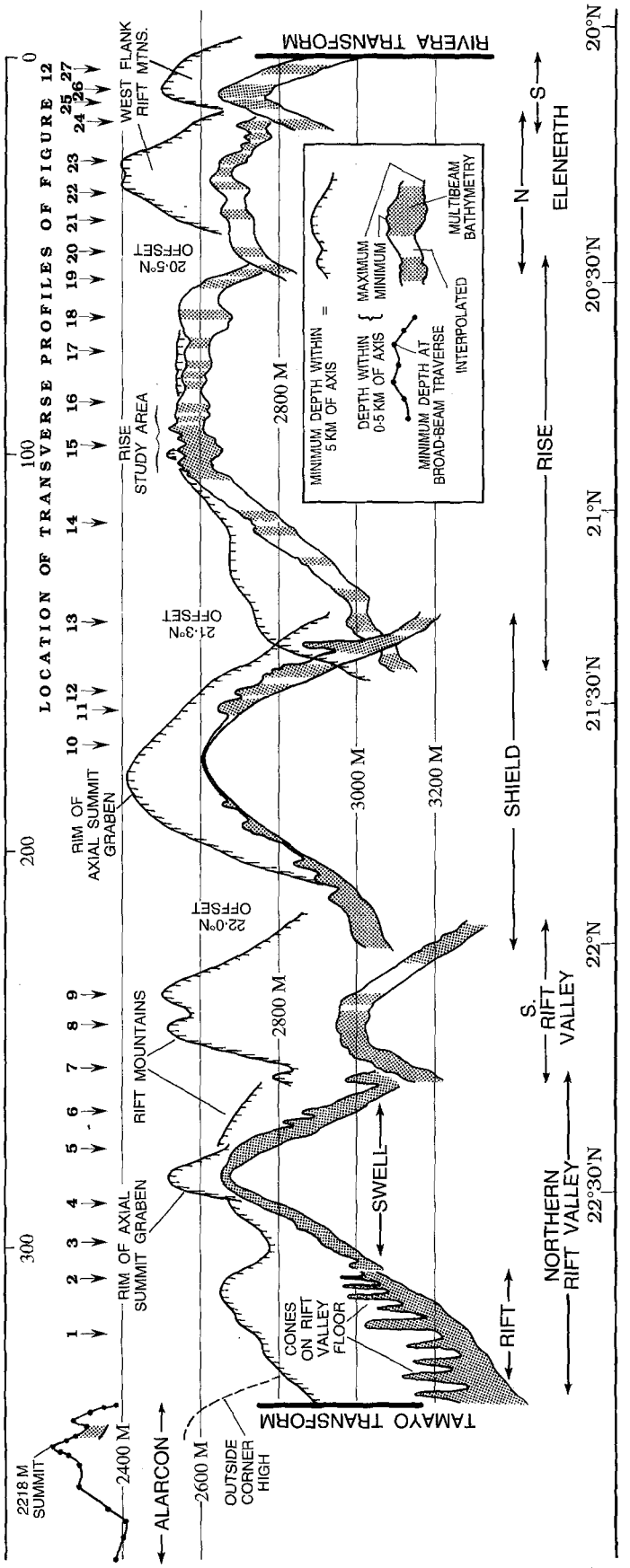

Fig. 11. Longitudinal profile of the risecrest, projected normal to the spreading direction with a 100× vertical exaggeration.

coalesced cones, which are supported by the crust of the rift valley floor and may be preserved as relief features on the rise flanks if they survive burial by lava on marginal parts of the rift floor or dissection by faulting at the rift walls. These "medial ridges", "central highs", or "central volcanic ridges" have different origins and fates from the broader "axial ridges" typical of the fast-spreading EPR, which are buoyed up by the low density of hot rock at the spreading center, and are not maintained as the crust moves off the axial zone and subsides (Madsen *et al.,* 1984; Wang and Cochran, 1993). The crests of many axial ridges have linear depressions called "axial summit grabens" (Lonsdale, 1977a) or "axial summit calderas" (Haymon *et al.,* 1991), formed by subsidence of the outcrop of volcanic rift zones following withdrawal of magma from subaxial chambers or following superficial extension above and ahead of noneruptive dike intrusions (Rubin and Pollard, 1988). Typical axial summit grabens on fast-spreading parts of the EPR are 50–1000 m wide and 5–100 m deep (e.g. Macdonald and Fox, 1988; Lonsdale, 1989b). Some medium-spreading rise segments have crestal ridges or elongate shield volcanoes that are as large as axial ridges, but are probably volcanic constructions of thickened crust supported by the strength of the axial lithosphere, making them candidates for preservation as topographic features of the rise flanks (Kappel and Ryan, 1986; Macdonald *et al.,* 1992). Most of these elongate shields are split by grabens larger than those along the crests of axial ridges, and probably formed by episodic collapse of the inflated volcanoes. Examples of the distinctive shield-splitting grabens have been referred to previously as "inner rifts" (Karsten *et al.,* 1986), "elongate summit depressions" (Kappel and Ryan, 1986), "axial valleys" (Kappel and Normark, 1987) and "axial grabens" (Macdonald *et al.,* 1992).

Pacific-North America segments

The two spreading axes that intersect Tamayo transform have strikingly different morphologies and axial depths, as noted by Lewis (1979) and illustrated by comparing profiles 1 and 2 of Figure 9. The long profile of the spreading axis steps down a full kilometer across the transform, from the region's shallowest neovolcanic zone along an axial ridge at the Alarcon segment to the region's deepest, along the floor of the Rift axial rift valley. Both structures contrast with sediment smothered Pacific-North America spreading axes further north within the Gulf, for example, at Guaymas Basin axes where 3–4 km-wide, 100–200 m-deep "axial troughs" bisect a sediment plain and sediment-doming intrusions take the place of central volcanic ridges (Lonsdale and Lawver, 1980).

Geomorphology of the Alarcon segment is known only from wide-beam echosounding and the single Seabeam traverse presented by Francheteau *et al.* (1983). This traverse, and adjacent published and unpublished wide-beam crossings (e.g., Lewis, 1979; Kastens *et al.,* 1979), indicate that the southern half of this segment has an axial ridge which stands 100–300 m above the faulted rise-flank terrain and has a 20–50 m-deep axial summit graben along much of its length. There are fairly steep along-axis gradients from a 2218 m-deep summit alongside the more axial of the Alarcon Seamounts. Profiles across the deeper northern half of the segment (e.g., Figure 3 of Ness *et al.,* 1991) lack a prominent axial ridge, and the magnetically defined spreading axis appears to occupy a small, shallow (~ 100 m-deep) rift valley.

The axial rift valley of the Rift segment is 500 m deep along most of its length, with both the valley floor and the crest of the rift mountains plunging toward Tamayo transform (Figure 11). This segment and its transform intersection is very similar in morphology to the northern part of the Gorda Ridge rift valley and its Blanco transform intersection (Malahoff, 1984; Clague and Holmes, 1987), though the total relief is somewhat less (Figure 8). Noteworthy points of similarity include an axial rift valley and inner rift that gradually widen as they approach the transform intersection, because for 20 km fault scarps on the western rift wall veer 5–10° away from the spreading axis; eastern rift terraces that extend further down the valley than the western terraces (which are truncated by the transform valley), and curve into an intersection high situated northeast of the spreading center-transform junction, i.e., on its outside corner; and a neovolcanic zone of rather isolated volcanic cones, changing with 10 km of the intersection to a narrow continuous volcanic ridge with a tip that curves part-way around a nodal basin. A submersible dive at the end of the EPR neovolcanic zone (Gallo *et al.,* 1984) found evidence of recent eruptions on this volcanic ridge and beyond its tip, in a band that extends past the axis of Tamayo transform and part-way up the transform-parallel scarp at the end of the outside corner high. A Deep Tow near-

bottom traverse of the rift valley 12 km from the transform (located on Figure 8) found the youngest volcanism to be on a ridge displaced west of the center-line of the inner rift (Macdonald *et al.*, 1979), and just further south (e.g., on profile 1 of Figure 12) the center-line is occupied by a narrow slot or cleft that is probably a collapse graben, and is closed off by one of the larger axial volcanic cones, a 300 m-high peak 1.5 km in diameter with a crater in its summit. In addition to the crude alignment of cones that defines the spreading axis along the southern half of this segment, other intact and faulting-modified cones can be recognized at the margins of the inner rift and on the rift terraces.

Spreading segments near Pacific-North America-Rivera triple junctions

The axis of the Swell segment occupies the same Northern Rift Valley as the Rift axis, being offset from it only by a tiny (1 km) left step at 22.6° N (Figure 8). The two segments were initially distinguished petrologically, with geochemical differences indicating that magma erupted at the Swell axis was produced by a greater degree of partial melting than at the Rift axis (Bender *et al.*, 1984; Bender and Langmuir, 1985). Petrologic evidence for enhanced melt supply is consistent with multibeam bathymetry of the axis. The "swell" is an elongate shield volcano with a rifted crest that rises above the rift valley walls for 10 km. It is asymmetrically located along the eastern side of the rift valley, and flows from the summit area have overtopped the eastern wall to spread across the adjacent rift mountains, where they are cut by fractures of the northern rupture zone (Figure 6). Identification of these young fractures as part of the North America-Rivera plate boundary implies that the northern half of the Swell segment now has a Pacific-North America axis, the southern half a Pacific-Rivera axis. About 10 km north of the triple junction the eastern valley wall emerges from its lava cover as the rifted volcanic swell narrows to a low ridge near the midline of a shallow fairly symmetric axial rift valley (profiles 3 and 4, Figure 12). South of the present triple junction the floor of the Northern Rift Valley deepens rapidly, and its central volcanic high is a curving row of coalesced volcanic cones.

The Southern Rift Valley segment, inferred to be a disoriented part of the Pacific-Rivera boundary, is described separately from the other parts because it was on the Pacific-North America boundary until the recent jump of the triple junction. It is structurally similar to the Northern Rift Valley, though the axial rift valley is only 6 km wide, narrowing at the northern end because the western valley wall converges obliquely with the axis. The deeper southern half of the rift valley is bounded on the east by tectonically rotated inter-rift plateaus at the 22.0° N offset. Only 15 km of the Southern Rift Valley segment has an axial rift valley bounded on both sides by undeflected rift mountains, with crestal depths near 2500 m, 500 m shallower than the adjacent valley floor. At the summit of the humped long profile (Figure 11), the central volcanic ridge near the midline of the valley floor is a small elongate swell split by a narrow graben (profile 8, Figure 12), but unlike the Northern Rift Valley the summit of this swell is much deeper than the rim of the rift valley. At profile 9 (Figure 12) the central volcanic ridge is a row of coalesced cones.

Pacific-Rivera segments

The straight, orthogonally spreading portion of the Shield segment (Figure 13) is 45 km long, and throughout this length the axis occupies a graben that splits the crest of a 20 km-wide elongate shield volcano. The northern part of the shield is dissected by close-spaced fault scarps, but in the summit region, asymmetrically near the southern end, there is little superficial evidence of faulting outside the graben except for a pair of inward-facing scarps 4.5 km off-axis (Profile 10, Figure 12). The southern end of the shield has a cluster of secondary volcanic cones and shields which have probably produced lava flows that have buried some fault scarps. The shield-splitting graben is 170–220 m deep in its straight central section, with a constant 2 km width except around 21°38′ N where it widens to accommodate a small left step of the axis. Most of the graben floor has a smooth, horizontal transverse profile, plunging along-axis at 10 m/km from a broad summit around 21°35′ N, which is in the middle of the segment but near the point where the southern half of the axis begins to curve into the large 21.3° N offset. At this point, near profile 11 (Figure 12), the shield-splitting graben broadens rapidly as its rims deepen, and central volcanic ridges occur in its axis, so that at profile 12 the cross-section resembles that of a shallow, rather asymmetric, axial rift valley. Near the southern tip of the axial rift zone the valley deepens into a 5 km-wide trough between plateaus of severely rotated abyssal hills. At the northern end of the elongate

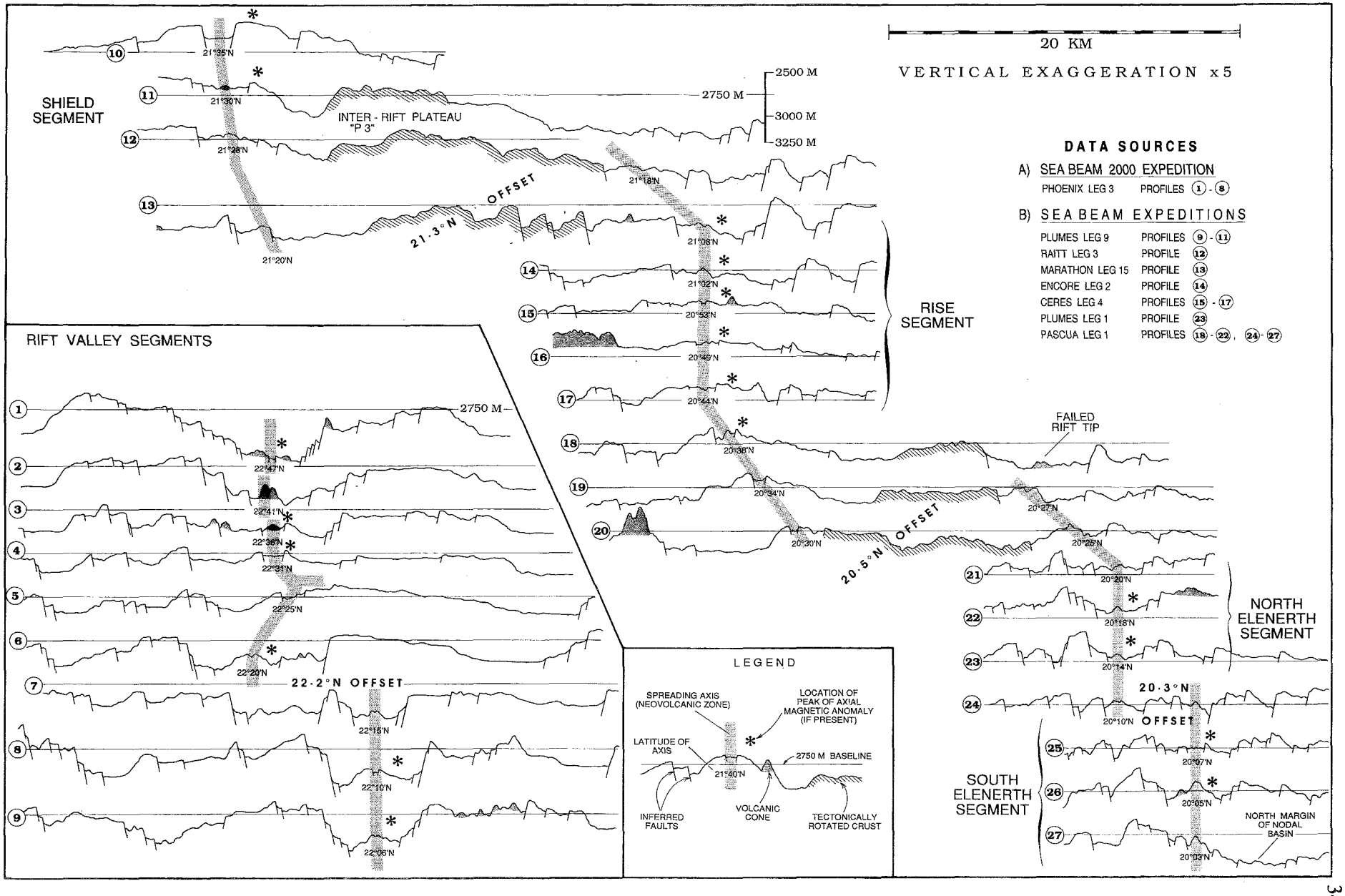

Fig. 12. Bathymetric transects of the risecrest from the narrow central beam of multibeam sonar traverses, projected parallel to the spreading direction and located on Figures 5, 8, 13, 14, and 15. Location of faults, tectonically rotated crust and volcanic peaks is inferred from the full swath of data.

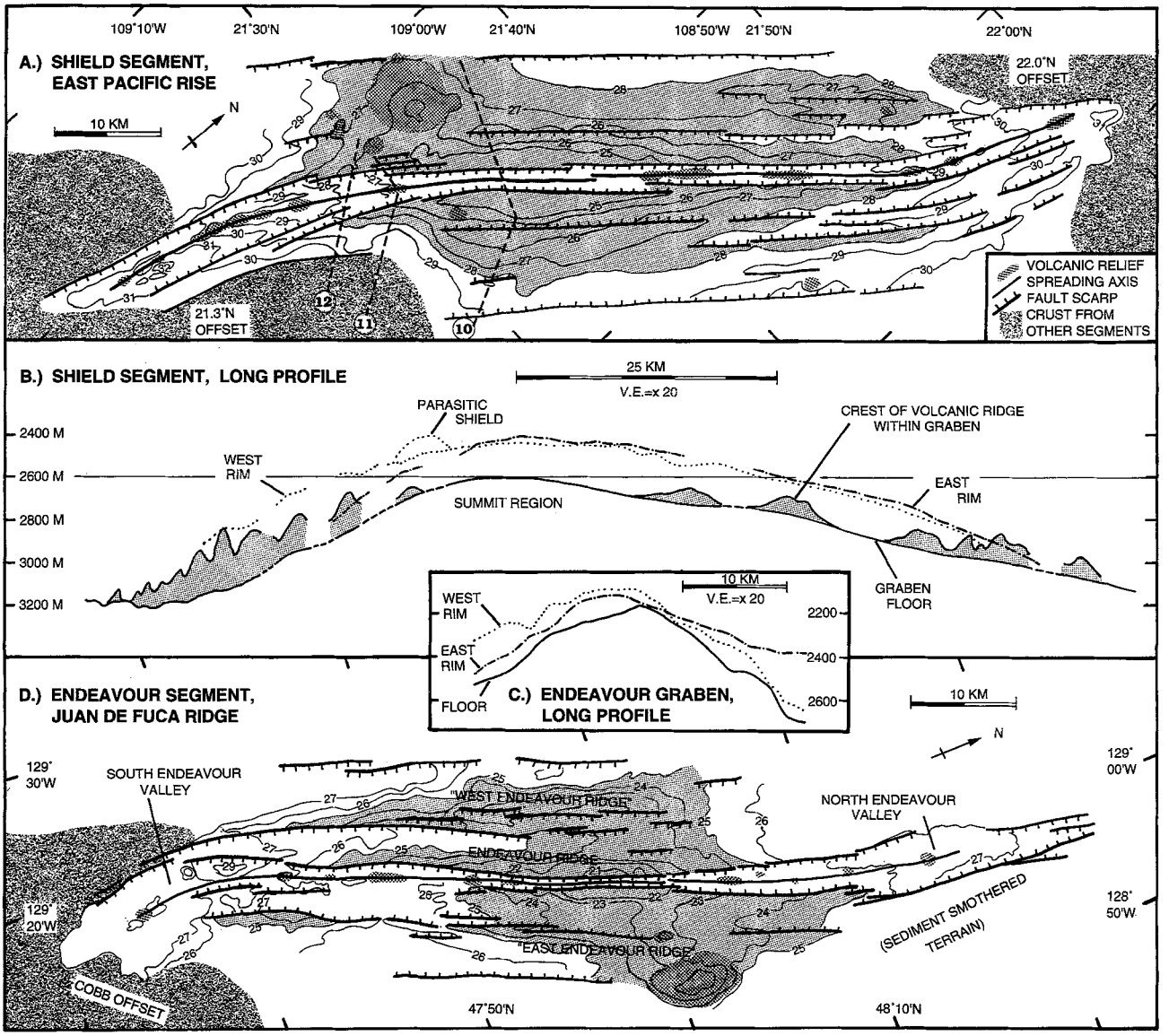

Fig. 13. Comparison of Shield segment on the EPR and Endeavour segment on the Juan de Fuca Ridge. Bathymetric interpretation of the latter is from Karsten *et al.* (1986) and Barone and Ryan (1988). Breaks in the long profile of Shield segment indicate gaps in Seabeam coverage; dashed lines locate profiles 10, 11 and 12 of Figure 12.

shield volcano the graben flares open as the axis curves into the 22.0° N offset; the structure is a smaller scale mirror-image of the southern end, except that the northern tip of this neovolcanic zone is marked by a row of small volcanic cones across a shallow basin (Figure 13), rather than by a deep trough.

The Rise segment has a northern half where a discontinuous central volcanic ridge lies within a northward-deepening 5–7 km wide axial rift valley (e.g., profiles 13 and 14, Figure 12) that curves into the 21.3° N offset and a southern half where the neovolcanic zone occupies the collapsed crest of a 6 km-wide axial ridge 200–300 m higher than the adjacent seafloor (e.g., profiles 17–19, Figure 12). In the transitional RISE Area of active hydrothermal venting and intensive near-bottom study at 20°49′ N–20°55′ N, a low (100 m-high) axial ridge has a shallow 2–3 km-wide fault-bounded summit depression in which most of the 100 m of local relief represents pillow ridges or cones and collapsed lava lakes (Francheteau *et al.*, 1981; Luyendyk and Macdonald, 1985). The Larson seamount chain extends west (260°) from this axial hydrothermal area; it includes a cluster of small pillow cones on crust only 0.2–03 m.y. old,

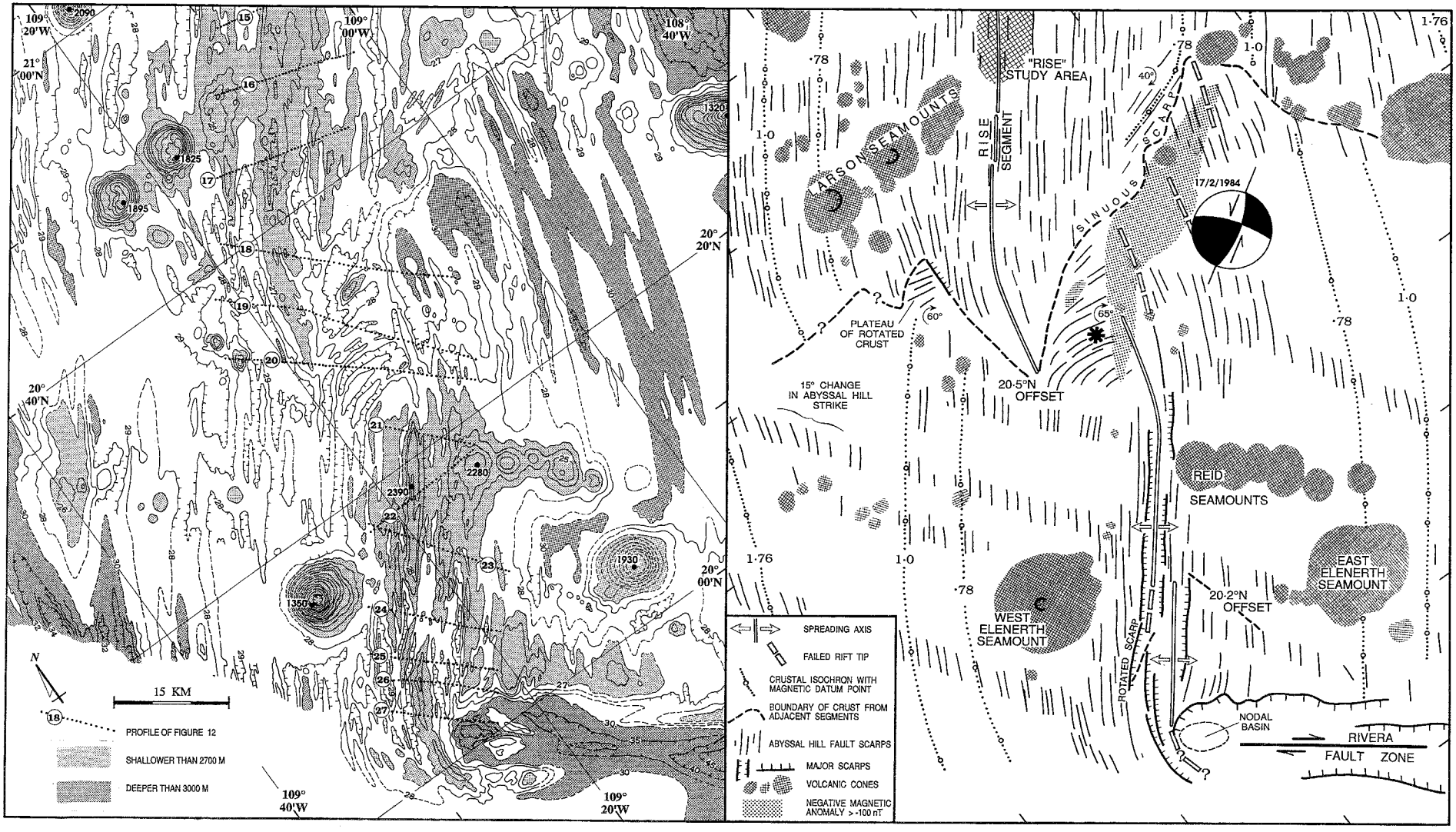

Fig. 14. The EPR crest around the 20.5° N offset and the western end of Rivera transform. Bathymetry at 100 m contour interval, in left panel, is mainly from multibeam surveys (see Figure 2 for track coverage) with broken contours interpolated using conventional soundings. Crustal structure and age (right panel) is inferred from bathymetric and magnetic data. Numbers (degrees) enclosed by curving arrows signify amount and direction of tectonic rotation of abyssal hill lineations. The asterisk is where the U.S. Geological Survey located a 17/2/1984 earthquake that was probably caused by left-lateral strike-slip faulting, as shown by the representation of the centroid moment tensor solution (Dziewonski, *et al.*, 1984).

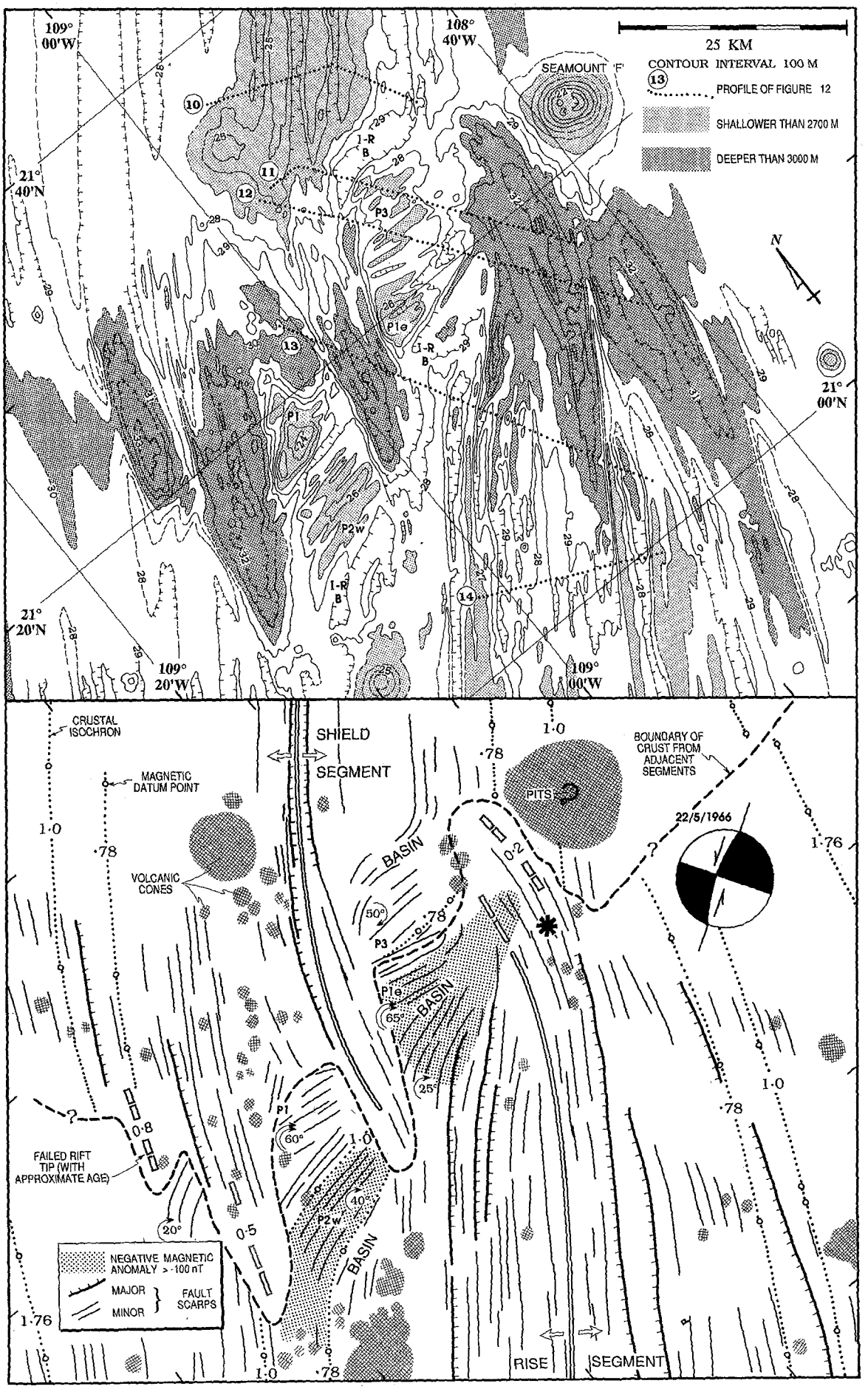
109° 00'W
108° 40'W
25 KM
CONTOUR INTERVAL 100 M
PROFILE OF FIGURE 12
SHALLOWER THAN 2700 M
DEEPER THAN 3000 M
SEAMOUNT 'F'
21° 40'N
21° 00'N
21° 20'N
109° 20'W
109° 00'W
N
1-R
B
P1
P1e
P2w
P3
CRUSTAL ISOCHRON
MAGNETIC DATUM POINT
SHIELD
SEGMENT
VOLCANIC CONES
BASIN
PITS
BOUNDARY OF CRUST FROM ADJACENT SEGMENTS
22/5/1966
FAILED RIFT TIP (WITH APPROXIMATE AGE)
NEGATIVE MAGNETIC ANOMALY > -100 nT
MAJOR
MINOR
FAULT SCARPS
RISE
SEGMENT

and two cratered 20 km^3 shield volcanoes on 0.4–0.7 Ma crust (Lonsdale, 1991).

The North Elenerth segment has a shallow axial rift valley (profiles 21–23, Figure 12) with west-flank rift mountains that form the shallowest parts of the risecrest between Rivera and Tamayo transforms, except for the summits of volcanoes that are slightly further off-axis, in the Reid seamount chain on the east flank and the much higher West and East Elenerth Seamounts (Figure 14). Just north of profile 21 the west flank rift mountains end abruptly as the North Elenerth neovolcanic zone emerges from its rift valley. It curves into the 20.5° N offset as a low volcanic ridge on the west side of an elongate basin, which is bisected by an alignment of volcanic cones and ridges labeled "failed rift tip" in Figures 14 and 12 (profile 18).

At the south end of the North Elenerth rift valley its western boundary scarp becomes oblique to the spreading direction. A possible explanation is that this "rotated scarp" (Figure 14) has been deflected by northward propagation of the South Elenerth axis, which occupies a low volcanic ridge in the midline of an adjacent, overlapping axial rift valley. Attenuation of seismic shear waves recorded at the central volcanic ridge indicated to Reid *et al.* (1977) that the spreading axis is underlain by hot and perhaps molten rock. Most of the South Elenerth rift valley is highly asymmetric, and the high western boundary scarps and the young crust of the western rift mountains extend past the Rivera transform intersection, curving eastward to partly enclose a nodal basin with a floor 500 m deeper than the crest of the central volcanic ridge. In contrast to the intersection of the Rift axis with Tamayo transform (Figure 8), but very like the intersection of the Juan de Fuca axis with Blanco transform (Embley and Wilson, 1992), the central volcanic ridge does not curve around this nodal basin, but ends abruptly near where the western rift wall begins to curve (at profile 27, Figure 12). The observation that the rift mountains extend past the transform intersection, whereas the volcanic ridge does not, could be explained by a recent retreat of the axial rift zone, or more plausibly by inferring that the crust-accreting rift zone still overshoots past the intersection, but lacks topographic expression because most lava erupted from the overshot part flows laterally into the nodal basin instead of piling up at a volcanic ridge.

It is evident from Figure 12 that Pacific-Rivera spreading axes, even without considering those within the Rivera transform system, display as much variation in structural geomorphology as the Pacific-North America axes. Some segments are so similar to previously described parts of other medium-spreading rises that my starting point for discussing the causes of variation in their risecrest relief will be interpretations based on observations of these other rises.

Shield segment resembles Cleft (a.k.a. Southern Symmetric), Split Volcano (a.k.a. Northern Symmetric) and especially Endeavour segment on the Juan de Fuca Ridge (Kappel and Ryan, 1986; Johnson and Holmes, 1989). Shield and Endeavour segments both have middle regions where a narrow graben splits an elongate shield volcano, and distal regions where the graben widens to a broader rift valley with a central volcanic ridge (Figure 13). The most recent phase of shield-building volcanism at the Endeavour segment was limited to a shorter fraction of the axis, building the feature known as Endeavour Ridge. The graben which splits this ridge, thoroughly studied by Barone and Ryan (1988), differs from its EPR counterpart in having a shorter constant-width portion, steeper longitudinal gradients away from the hump at the summit of the graben floor, and greater variation in the height of its walls. The shallow rift valleys at the crests of the Elenerth segments and the northern part of the Rise segment may have a Juan de Fuca Ridge counterpart in the Vance (a.k.a. Shingle Ridge) segment (Kappel and Ryan, 1986; Johnson and Holmes, 1989), and closely resemble the asymmetric valley at 86° W on the Galapagos Rift segment of the Cocos-Nazca rise (Lonsdale, 1977b; van Andel and Ballard, 1979). The axial ridge along the southern half of the Rise segment appears similar to ridges along other parts of the Cocos-Nazca axis, closer to the Galapagos Islands (Schilling *et al.*, 1982).

Fig. 15. The EPR crest around the 21.3° N offset. Bathymetry in upper panel is mainly from multibeam surveys (see Figure 2 for track coverage) with broken contours interpolated using conventional soundings. Crustal structure and age (lower panel) are inferred from bathymetric and magnetic data. Numbers (degrees) enclosed by curving arrows signify amount and direction of tectonic rotation of abyssal hill lineations; double arrows indicate more than one rotation episode. The asterisk is where Sykes (1970) located the 22/5/1966 earthquake for which his focal mechanism solution is presented as a conventional projection of the focal sphere; the inferred direction of left-lateral motion is indicated by arrows. (Note that Sykes chose the northwest-striking nodal plane as the fault plane, and therefore interpreted this earthquake as the result of right-lateral transform faulting).

The Nontransform Offsets

Origin and early history

As previously noted, the rise-flank record indicates that the left steps of the risecrest south of Tamayo transform originated and grew since 2.6 Ma as adjustments of the plate boundary to clockwise rotation of spreading direction, especially during the Early Pleistocene on the Pacific-Rivera boundary. The different offset lengths were a direct geometric result of the varying lengths and rotations of the spreading segments they separated, the largest (21.3° N) offset developing between the two longest, most rotated, segments.

The directions and speeds at which the nontransform offsets have migrated along the risecrest are recorded by the azimuths of their rise-flank trails, identifiable by misalignments of magnetic stripes and as seams between abyssal hills with different strikes. The trails mapped in Figures 3 and 4 indicate that until about 0.5 Ma the three northern offsets migrated southward at a rather steady and uniform speed, equal to 40% of the spreading rate. The 21.3° N offset also moved slowly southward while it was a small (< 5 km) left step, then accelerated soon after the Jaramillo event until stagnating at about 0.5 Ma. Much of the trail of the 20.5° N offset is obscured by seamounts on the east flank, and lies within a gap in Seabeam coverage on the west flank, but this offset seems to have migrated slowly north until early in the Brunhes epoch, when it reversed direction. Both the northward movement before 0.5 Ma and the steadiness of its migration since that time contrast with behavior of the other offsets, where more erratic recent histories can be interpreted from risecrest geomorphology.

Structural interpretation and recent history

Bathymetry and an interpretation of the crustal age and structure at the 5 principal offsets of the risecrest between Tamayo and Rivera transforms are shown in Figures 5, 14, and 15. Those at 22.2° N and 20.2° N are merely small left steps of axial rift valleys, lacking the typical features of equally short offsets elsewhere on the EPR, such as overlapping rift zones that curve toward each other around overlap basins. Recent renewal of southward migration of the 22.2° N offset is inferred from the 25° clockwise rotation of the western valley wall at the end of the Southern Rift Valley, alongside the apparently propagating tip of the Swell segment. The three larger offsets do resemble equally large shear zones migrating along fast-spreading parts of the EPR, e.g., the nontransform offsets at 2.0° N, 2.8° S and 20.7° S (Lonsdale, 1989c; Perram *et al.*, 1993). Essential similarities include (1) overlapping, inward-curving rift zones separated by patches of abyssal hills with the highly oblique azimuths diagnostic of tectonic rotation: (2) inter-rift plateaus and shallow basins, evidence that lateral rotation of inter-rift crust was accompanied by vertical displacements; (3) continuity of rotated abyssal hills in inter-rift sites with unmodified coeval hills on the rise flanks, the intervening bend in structural lineations indicating internal deformation of the lithosphere alongside the tip of one of the rift zones (the propagating one); and (4) evidence for episodic, often short-lived reversals in the direction of along-axis migration.

The 22.0° N, 21.3° N and 20.5° N offsets also resemble, to varying degrees, two previously studied nontransform offsets at 20–30 km left steps of other intermediate-rate spreading centers: the steadily migrating 95.5° W offset of the Cocos-Nazca rise, also called a propagating rift system (Hey *et al.*, 1986), and the Cobb offset on the Juan de Fuca ridge, known as a dueling propagator because of its frequent alternations of migration direction (Johnson *et al.*, 1983). The most thorough investigations into mechanisms of abyssal hill rotation and causes of inter-rift uplift and subsidence, resulting in dynamic models that should be applicable and testable at the Pacific-Rivera risecrest, have been made at the 95.5° W offset. Searle and Hey (1983) and Kleinrock and Hey (1989a) show that as westward migration of this offset transfers lithosphere from the Cocos to the Nazca plate through a broad right-lateral shear zone, the rotating crust first subsides into the inter-rift basin called de Steiguer Deep, then is uplifted as the inter-rift plateau called de Steiguer Ridge. They postulate that shearing proceeds by the process of bookshelf faulting, in which the right-lateral shear stress is accommodated by antithetic left-lateral motion along preexisting faults which bound increasingly oblique abyssal hills, and that with certain geometries of preexisting faults this process can itself cause extension and hence inter-rift subsidence, followed by compression and uplift. Kleinrock and Hey (1989a) suggest that major inter-rift extension, large enough to create de Steiguer Deep, may depend on the retreating spreading segment and its abyssal hills being oblique to the spreading direc-

tion; indirect evidence for this suggestion is the lesser development of inter-rift basins at the 21.3° N and 20.5° N Pacific-Rivera offsets, where there is no such obliquity. Direct evidence for the antithetic strike-slip faulting predicted by their model comes from focal mechanisms of earthquakes at each of the Pacific-Rivera offsets, though epicenter determinations are not precise enough to locate them definitively in the rotating inter-rift zone. Of the two possible fault motions that could cause the focal mechanism solutions plotted in Figures 5, 14 and 15, the more plausible is left-lateral slip along northeast-striking planes (Lonsdale, 1991; Wetzel *et al.,* 1993). These planes parallel some of the rotated fault scarps mapped in the inter-rift shear zones, whereas the alternative right-lateral interpretation would imply transform faulting that is oblique to the spreading direction and leaves no superficial fault traces.

The Pacific-Rivera offset most similar in its present structure to the 95.5° W propagating rift system is the one at 20.5° N (Figure 14), which has been migrating in the same direction (southward) for the longest time. Even the steady migration of the 95.5° W offset proceeds by episodic failure of the inward-curving tip of the retreating axis, leaving a trail of adjoining and coalescing rift valleys that head at a sinuous scarp (Wilson, 1990), and the 20.5° N offset has a similar eastflank trail of deeps containing failed tips of the retreating Elenerth segment. However, magnetic and bathymetric lineations indicate that crust at the crest of the 20.5° N sinuous scarp originated at the propagating (Rise) segment, rather than being rotated crust transferred from the other flank of the retreating segment, as in the 95.5° W type example. At 20.5° N and at the other Pacific-Rivera offsets, the rotated abyssal hills in inter-rift sites are completely truncated by failed rift tips, rather than extending down the rise flanks as continuous bands at the margins of inner pseudofaults (Hey *et al.,* 1986). As the transferred lithosphere leaves an inter-rift shear zone past the tip of a retreating EPR axis, the rotated structural fabric is probably obliterated, overprinted or hidden by renewed axial fissuring, normal faulting and perhaps volcanism. A deep negative magnetic anomaly over the zone of failed rift tips at the foot of the 20.5° S sinuous scarp (Figures 3 and 14) supports the inference of old (i.e., pre-Brunhes) crust that has been tectonically rejuvenated after transfer from the west flank.

Structural geomorphology of the 22.0° N and 21.3° N offsets (Figures 5 and 15) has more in common with the Cobb offset than with the 95.5° N offset, being dominated by the effects of recent reversals in propagation direction. In such dueling systems, some slabs of inter-rift crust get rotated repeatedly by more than one episode of rift propagation (Shoberg *et al.,* 1991), and some get shed from the axial inter-rift zone when the direction of rift propagation reverses, to leave isolated patches, usually plateaus, of rotated abyssal hills on the rise flanks (e.g., at the 2.0° N EPR offset, Lonsdale, 1989c). Rotated plateaus of this type even occur on the flanks of the 20.5° N offset (Figure 14), recording reversals in propagation direction prior to its current steadier migration.

At the 22.0° N offset (Figure 5), the northward retreat of the Southern Rift Valley axis which ended its period of steady southward migration is recorded by a 0.5 Ma failed rift tip 12 km west of the present axial rift valley. The failed tip is in a fault trough with an amphitheater-like head cut into the flank of the Shield segment, and probably floored by down-dropped Shield crust, though it is at the end of a southward-deepening rise-flank valley which extends the entire length of the Southern Rift Valley segment. The patch of Shield crust east of the failed propagator tip has curving abyssal hills, showing it had been rotated clockwise as much as 35° before its transfer to the west flank was arrested by retreat of the propagating rift tip. Subsequent renewal of southward propagation while the crust now forming the rift mountains was being accreted brought the rift tip slightly further south than at 0.5 Ma. Southernmost eruptions from the axial rift zone of the Southern Rift Valley may have built the mapped cluster of small volcanic cones (Figure 5), which resemble those described by Kleinrock and Hey (1989b) around the "initial volcanic tip" of the 95.5° W propagating rift. There is evidence that the southern end of the Southern Rift Valley is now in a phase of abandonment: the present axis occupies a trough like the one at the 0.5 Ma failed tip, and the overlapping Shield rift zone has recently lengthened northward, causing a 40° rotation of structures in the eastern rift mountains. Most of the rotated patch of rift mountains is only slightly shallower than the unrotated mountains to the north, but one ridge rises much higher, to within 2220 m of sea-level (Figure 5). This steep-sided ridge might be a fault-modified volcanic construction, a seamount accidentally trapped in an inter-rift setting like Endeavour Seamount at the Endeavour offset of the Juan de Fuca Ridge (Karsten *et al.,* 1986). Alternatively, it may be a small

patch of normally accreted crust that has been successively uplifted during repeated transfers between east and west rise-flanks while the 22.0° N offset oscillated north and south for the past 0.5 m.y.; this hypothesis is consistent with the better constrained interpretation of the larger, almost equally shallow inter-rift areas at the 21.3° N offset.

The western rise flank at the 21.3° N offset (Figure 15) has two amphitheater-headed fault troughs similar to the one 12 km off-axis at 22.0° N. They are inferred to contain tips of the Shield segment that failed after spasms of southward propagation at 0.8 Ma and 0.5 Ma. Following the 0.5 Ma event the tip of the Shield axis retreated 25 km northward, as the overlapping tip of the Rise segment advanced a similar distance northward to a position west of the Seamount F volcano. Most recently, renewed southward propagation of the shield rift zone has opened the 5 km-wide fault trough in which the present axis lies, and there has been a corresponding retreat of the Rise segment, the north tip of its central volcanic ridge near profile 11 (Figure 12) now being about 10 km south of its inferred former position. The cycles of rift propagation and retreat in both directions have caused variable tectonic rotation and uplift of patches of crust in the shear zone. For example, the pulse of southward propagation that ended about 0.5 Ma caused overlapped 1.0–0.78 Ma crust accreted to the west flank of the Rise segment to be rotated 40° and uplifted a few hundred meters to form a 2550–2750 m-deep plateau (P2 in Figure 15). It also overlapped, rotated and uplifted an existing inter-rift plateau (P1) developed on older crust by the 0.8 Ma propagation pulse. Plateau Pl had originally been rotated about 20°, judging from the curving lineations near the 0.8 Ma failed tip; by 0.5 Ma it had been rotated 60° clockwise, and uplifted to summit depths of 2350–2550 m. The most recent pulse of rapid southward propagation bisected plateau Pl, causing its eastern third (Ple in Figure 15) to spin a few more degrees clockwise; the central part of this rifted plateau was probably down-dropped to form the floor of the axial trough.

Conjectures on Relationships Between Magma Supply, Axial Relief, and Offset Migration

Structural contrasts between adjacent spreading segments on the same plate boundary are plausibly explained by differing rates of magma supply to the crustal accretion zone (e.g., Fox *et al.*, 1991). Spatial or temporal variations within a single segment can be attributed to the same cause, especially within the context of models that emphasize a punctiform magma supply to the linear axes (e.g., Macdonald *et al.*, 1988). The sensitivity of risecrest structure to variations in magma budget is probably greatest at intermediate spreading rates, near the 60–70 mm yr^{-1} rate at which the transition from rifted to unrifted risecrests usually occurs (Small and Sandwell, 1989).

The concept of topographic sensitivity to melt supply would imply an above-average supply rate to the Alarcon segment and part of the Rise segment, because their axial ridges imply large, laterally continuous axial magma chambers. Below-average magma supply is inferred for the Rift and Southern Rift Valley segments, where axial rift valleys indicate relatively strong lithosphere lacking large or permanent magma chambers. The Rift neovolcanic zone (Figure 8) has a volcano-studded topography much like that on many segments of the slow-spreading Mid-Atlantic Ridge, where it is inferred to be produced by small, infrequent eruptions from temporary, isolated magma pockets (Smith and Cann, 1992). The split shield-volcano topography of the Shield segment may be diagnostic of a highly episodic magma supply, with voluminous shield-building axial volcanism alternating with periods of low-supply tectonic stretching (Kappel and Ryan, 1986). Lewis (1979) suggested that the rift mountains and rise-flank ridges of the Northern Rift Valley are also derived by tectonic splitting of axial volcanoes, like the one he recognized at the Swell segment. With more complete surveying, however, I infer that the episode of voluminous eruption that recently built a large shield volcano within part of the Northern Rift Valley probably has a special local cause, namely the jump of the RRR Pacific-North America- Rivera triple junction to the Swell segment. Evidence of a causal connection is that the locus of maximum eruption at the summit of the axial shield volcano is exactly where the main fractures of the northern rupture zone intersect the EPR axis, and is shifted toward the eastern side of the rift valley. Perhaps lithospheric extension along the rupture zone has enhanced and diverted the decompression melting that supplies magma to the EPR plate accretion zone. This hypothesis is consistent with the petrologic evidence that Swell magmas were produced by higher degrees of partial melt than magmas erupted elsewhere in the Northern Rift Valley. Perhaps the intersection of rupture zone fractures

merely increased the permeability of the crust and eased magma egress. I think it unlikely that the Swell shield volcano is merely typical of the magmatic phase of a non-steady-state rift valley, though there is the alternative possibility that the triple junction shifted to this site because it entered a lithosphere-weakening magmatic phase, and I favor a tectonic-uplift interpretation for the walls of the Northern Rift Valley.

Testing any of the topography-based inferences of the previous paragraph requires additional measurements of other indicators of a variable magma supply. Variation in crustal thickness would be a fairly direct indicator. Refraction results of McClain and Lewis (1980) do indicate that crust flooring the rift valley at the Rift segment is thinner than average, and thins toward Tamayo transform as the valley deepens, but there are few comparable measurements from other segments. Volcanic seamounts that grew in the plate boundary zone, as many on this part of the EPR seem to have done (Lonsdale and Batiza, 1980; Allen *et al.,* 1987), represent local thickenings of the crust at sites of above-average melt delivery to the axial zone. Cratered shield volcanoes ~1 km high (the seamounts located on Figure 3) occur on crust younger than 0.78 Ma at the Alarcon and Rise segments, both of which have axial ridges, and at the Elenerth segment, which has the shallowest risecrest between Rivera and Tamayo transforms (Figure 11). There are no such seamounts on crust accreted in the past 1 m.y. at the "magma-starved" rift valley segments. The clearest association of seamount volcanism with enhanced axial magmatism is the intersection of the Larson seamount chain, the product of a volcano-building melting site that has persisted for more than 0.5 m.y., with the summit of the Rise axial ridge and with the active, magma-fueled RISE hydrothermal field. The 260° azimuth of this seamount chain, shared by two other young west-flank chains (Figure 3), tracks the motion of the Pacific plate with respect to melt anomalies that are constrained to underlie the westward-drifting spreading axis (Lonsdale, 1991); the southeasterly striking chains on the young east flank (Figure 3) parallel motion of Rivera microplate relative to similar features of the sub-axial asthenosphere. In general, what evidence there is from seismic refraction experiments and from mapped seamount distribution corroborates the inferences of axial magma budgets based on risecrest topography.

It has been suggested (e.g., Macdonald *et al.,* 1988) that inter-segment variation in magmatic budgets also controls the direction of offset migration, with well supplied segments that have shallow risecrest topography lengthening at the expense of adjacent magma-deficient segments. Some parts of the EPR provide evidence for the contrary view that offset migration controls the magmatic budget, with segments that shorten because of offset migration acquiring shallow, "robust" topography because their magma supply is distributed along a decreasing length of accreting plate boundary (Lonsdale, 1985). For the past 0.5 m.y. the well supplied Alarcon segment has been constrained by long transform offsets to maintain a constant length, but the Rise segment lengthened by about 30%. It is plausible that this expansion, produced by reversals in migration direction at the bounding 21.3° N and 20.5° N offsets, was caused by the enhanced magma supply evidenced by the seamount chains and the axial ridge topography. The very recent expansion of the Shield segment, at the expense of the Southern Rift Valley and the rifted part of the Rise axis, could be associated with the magmatic pulse that built the young (almost unfractured) axial shield volcano on this segment. Variable magma supply to competing spreading segments is surely not the only control on offset migration, however. The systematic southward migration of all but one of these left-stepping offsets prior to 0.78 Ma may be better explained by the greater vulnerability of one of the rise flanks (the fast-moving Pacific plate one) to rift propagation (Lonsdale, 1994).

Full understanding of the structural geomorphology of this rise would mean knowing how changing patterns and identities of the plate boundaries, and changing routes and rates of magma supply, have affected risecrest relief and disrupted the rise flanks. For now, most of the possible interrelationships are conjectural.

Principal Conclusions of this Study

1. The EPR in the mouth of the Gulf of California includes parts of both the Pacific-North America and the Pacific-Rivera boundaries. The triple junction between the three plates has changed its tectonic type and its position during the Pleistocene, and is now an RRR junction 60 km south of Tamayo transform. The western part of the North America-Rivera boundary includes zones of lithospheric rupture that cross-cut abyssal hill terrain on the eastern flank of the rise; the

North America-Rivera Euler pole is near the east end of these rupture zones.

2. Movement of the North America plate is now a major force driving the anticlockwise rotation of the Rivera microplate, which has changed its motion significantly during the past 2.6 m.y. in response to changes in surrounding plates. The microplate slowed markedly about 1.5 Ma, when its southern boundary evolved from a broad shear zone between interacting Rivera and Mathematician microplates to a Pacific-Rivera transform fault zone.
3. Clockwise change in the direction of Pacific-Rivera spreading rapidly produced a staircase of spreading segments, separated by left-stepping nontransform offsets similar in structure to large NTOs on fast-spreading parts of the EPR. Migration of these offsets has proceeded by rift propagation into abyssal hill terrain, which is internally deformed by bookshelf faulting and uplifted into plateaus of rotated crust. The deformation is accompanied by antithetic (left-lateral) strike-slip seismicity. As rotated crust leaves the inter-segment shear zones past retreating rise axes it is overprinted by new structural lineations, unless reversals in migration direction cause it to be shed onto the rise flank as intact rotated plateaus.
4. Pacific-North America spreading axes include one that originated as an intra-continental rift between Baja California and the mainland, and others (south of Tamayo transform) that evolved from a Pacific-Rivera axis which propagated past now-extinct Pacific-North America axes. Pleistocene changes in Pacific-North America spreading direction were smaller than on the Pacific-Rivera boundary, so the intersegment offsets are shorter.
5. Pacific-North America and Pacific-Rivera spreading segments show a wide range of structural morphology, from axial rift valley to split shield volcano and axial ridge. All types have counterparts described on other medium-spreading rises, especially the Juan de Fuca Ridge. The variation is probably caused by inter-segment differences in magma supply rates.

Acknowledgments

For help in data collection I thank the crews and scientific parties on Scripps Seabeam Expeditions Raitt (leg 3), Plumes (leg 6), Encore (leg 2) and Phoenix (leg 3), and on many additional expeditions led by other scientists. My field work and data analysis was supported by the U.S. National Science Foundation (grant OCE 91-16493), the U.S. Navy Office of Naval Research, and the state of California. Permission for scientific research within their exclusive economic zone was graciously provided by the Government of Mexico.

References

Alt, J. C., Lonsdale, P., Haymon, R. and Muehlenbachs, K., 1987, Hydrothermal Sulfide and Oxide Deposits on Seamounts near 21° N, East Pacific Rise, *Geol. Soc. America Bull.* **98**, 157–168.

Argus, D. F. and Gordon, R. G., 1990, Pacific-North American Plate Motion from Very Long Baseline Interferometry Compared With Motion Inferred From Magnetics Anomalies, Transform Faults, and Earthquake Slip Vectors., *J. Geophys. Res.* **95**, 17315–17324.

Atwater, T., 1970, Implications of Plate Tectonics for the Cenozoic Evolution of Western North America, *Geol. Soc. Am. Bull.* **81**, 3513–3536.

Atwater, T., 1989, Plate Tectonic History of the Northeast Pacific and Western North America, *Geology of North America, Geol. Soc. Am.*, Boulder, CO., N, 21–72.

Atwater, T. M. and Mudie, J. D., 1973, Detailed Near-Bottom Geophysical Survey of the Gorda Rise, *J. Geophys. Res.*, **78**, 8665–8686.

Ballard, R. D., Francheteau, J., Juteau, T., Rangin, C. and Normark, W., 1981, East Pacific Rise at 21° N: The Volcanic, Tectonic, and Hydrothermal Processes of the Central Axis, *Earth Plan. Sci. Letts.* **55**, 1–10.

Batiza, R., Fornari, D. J., Vanko, D. A. and Lonsdale, P., 1984, Craters, Calderas, and Hyaloclastites on Young Pacific Seamounts, *J. Geophys. Res.* **89**, 8371–8390.

Bender, J. F., Langmuir, C. H. and Hanson, G. N., 1984, Petrogenesis of Basalt Glasses from the Tamayo Region, East Pacific Rise, *J. Petrology* **25**, 213–254.

Bender, J. F. and Langmuir, C. H., 1985, The Tamayo Region of the EPR; Constraints on the TFE Model from Off-Axis Sampling (abstract), *EOS, Trans. Am. Geophys. Union* **66**, 1108.

Bourgois, J., Renard, V., Aubouin, J., Bandy, W., Barrier, E., Calmus, T., Carfantan, J., Guerrero, J., Mammerickx, J., Mercier de Lepinay, B., Michaud, F. and Sosson, M., 1988, La jonction orientale de la dorsale Est-Pacifique avec la zone de Fracture de Rivera au large du Mexique, *Comptes Rendus Acad. Sci. Paris* **307**, 617–626.

Cande, S. C. and Kent, D. V., 1992, A New Geomagnetic Polarity Time Scale for the Late Cretaceous and Cenozoic, *J. Geophys. Res.* **97**, 13917–13951.

Cande, S. C., Herron, E. M. and Hall B. R., 1982, The Early Cenozoic Tectonic History of the Southeast Pacific, *Earth Plan. Sci. Letts.*, **57**, 63–74.

Choukroune, P., Fox, P. J., Seguret, M., Francheteau, J., Needham, H. D., Juteau, T., Ballard, R. D., Normark, W., Carranza, A., Cordoba, D., Guerrero, J., Rangin, C. and Pastouret, L., 1981, Submersible Structural Study of

Tamayo Transform Fault: East Pacific Rise, 23° N (Project RITA), *Mar. Geophys. Res.* **4**, 381–401.

Clague, D. A. and Holmes, M. L., 1987, Geology, Petrology, and Mineral Potential of the Gorda Ridge, in Geology and Resource Potential of the Continental Margin of Western North America and Adjacent Ocean Basins – Beaufort Sea to Baja California, *Circum-Pacific Council for Energy and Mineral Resources, Earth Science Series* **6**, 563–580, Houston, Texas.

Cochran, J. R., Goff, J. A., Malinverno, A., Fornari, D. J., Keeley, C. and Wang, X., 1993, Morphology of a "Superfast" Mid-Ocean Ridge Crest and Flanks; the East Pacific Rise, 7°–9° S, *Mar. Geophys. Res.* **15**, 65–75.

Crouch, J. K., Bachman, S. B. and Shay, J. T., 1984, Post-Miocene Compressional Tectonics Along the Central California Margin, *Society of Economic Palaeontologists and Mineralogists Publ.* **38**, 37–54, Bakersfield.

de Mets, C., Gordon, R. G., Stein, S. and Argus, D. F., 1987, A Revised Estimate of Pacific-North America Motion and Implications for Western North America Plate Boundary Zone Tectonics, *Geophys. Res. Letts.* **14**, 911–914.

de Mets, C., Gordon, R. G., Argus, D. F. and Stein, S., 1990, Current Plate Motions, *Geophys, J. Int.* **101**, 425–478.

de Mets, C. and Stein, S., 1990, Present-Day Kinematics of the Rivera Plate and Implications for Tectonic in Southwestern Mexico, *J. Geophys. Res.* **95**, 21931–21948.

Dziewonski, A. M., Franzen, J. E. and Woodhouse, J. H., 1984, Centroid-Moment Tensor Solutions for January-March, 1984, *Phys. Earth Planet. Int.* **34**, 209–219.

Dziewonski, A. M., Franzen, J. E. and Woodhouse, J. H., 1986, Centroid-Moment Tensor Solutions for July-September 1985, *Phys. Earth Planet. Int.* **42**, 205–214.

Eissler, H. K. and McNally, K. C., 1984, Seismicity and Tectonics of the Rivera Plate and Implications for the 1932 Jalisco, Mexico, Earthquake., *J. Geophys. Res.* **89**, 4520–4530.

Embley, R. W. and Wilson, D. S., 1992, Morphology of the Blanco Transform Zone, Northeast Pacific: Implications for its Tectonic Evolution, *Mar. Geophys. Res.* **14**, 25–45.

Fox, P. J., Grindlay, N. R. and Macdonald, K. C., 1991, The Mid-Atlantic Ridge (31° S–34° 30′ S): Temporal and Spatial Variations of Accretionary Processes, *Mar. Geophys. Res.* **13**, 1–20.

Francheteau, J., Needham, H. D., Choukroune, P., Juteau, T., Seguret, M., Ballard, R. D., Fox, P. J., Normark, W. R., Carranza, A., Cordoba, D., Guerrero, J. and Rangin, C., 1981, First Manned Submersible Dives on the East Pacific Rise at 21° N (Project RITA): General Results, *Mar. Geophys. Res.* **4**, 345–379.

Francheteau, J. and Ballard, R. D., 1983, The East Pacific Rise Near 21° N, 13° N and 20° S: Inferences for Along-Strike Variability of Axial Processes of the Mid-Ocean Ridge, *Earth Plan. Sci. Letts.* **64**, 93–116.

Francheteau, J., Choukroune, P., Rangin, C. and Seguret, M., 1983, Bathymetric Map of the Tamayo Transform Fault, *Initial Reports DSDP* **65**.

Gallo, D. G., Kidd, W. S. F., Fox, P. J., Karson, J. A., Macdonald, K., Crane, K., Choukroune, P., Segurel, M., Moody, R. E. and Kastens, K., 1984, Tectonics at the Intersection of the East Pacific Rise with the Tamayo Transform Fault, *Mar. Geophys. Res.* **6**, 159–185.

Gente, P., Auzende, J. M., Renard, V., Fouqet, Y. and Bideau, D., 1986, Detailed Geological Mapping by Submersible of the East Pacific Rise Axial Graben Near 13° N, *Earth Plan. Sci. Letts.* **78**, 224–236.

Goldfarb, M. S., Converse, D. R., Holland, H. D. and Edmond, J. M., 1983, The Genesis of Hot Spring Deposits on the East Pacific Rise, 21° N, in Ohmoto, H. and Skinner, B. J. (eds.), *The Kuroko and Related Volcanogenic Massive Sulfide Deposits., Econ. Geol. Monograph* **5**, 184–197.

Gripp, A. E. and Gordon, R. G., 1990, Current Plate Velocities Relative to the Hotspots Incorporating the NUVEL-1 Global Plate Motion Model, *Geophys. Res. Letts.* **17**, 1109–1112.

Haymon, R. M., Fornari, D. J., Edwards, M. H., Carbotte, S., Wright, D. and Macdonald, K. C., 1991, Hydrothermal Vent Distribution Along the East Pacific Rise Crest (9°09′–54′ N) and its Relationship to Magmatic and Tectonic Processes on Fast-Spreading Mid-Oceans Ridges, *Earth Planet. Sci. Letts.* **104**, 513–534.

Hey, R. N., Kleinrock, M. C., Miller, S. P., Atwater, T. M. and Searle, R. C., 1986, Sea Beam/Deep-Tow Investigation of an Active Oceanic Propagating Rift System, Galapagos 95.5° W, *J. Geophys. Res.* **91**, 3369–3394.

Hey, R. N., Menard, H. W., Atwater, T. M. and Caress, D. W., 1988, Changes in Direction of Seafloor Spreading Revisited, *J. Geophys. Res.* **93**, 2813–2838.

Johnson, H. P., Karsten, J. L., Delaney, J. R., Davis, E. E., Currie, R. G. and Chase, R. L., 1983, A Detailed Study of the Cobb Offset of the Juan de Fuca Ridge: Evolution of a Propagating Rift, *J. Geophys. Res.* **88**, 2297–2315.

Johnson, H. P. and Holmes, M. L., 1989, Evolution in Plate Tectonics; the Juan de Fuca Ridge, in *The Geology of North America*, Geological Society of America, Boulder CO, vol. N, pp. 73–91.

Juteau, T., Eissen J. P., Francheteau, J., Needham, D., Choukroune, P., Rangin, C., Seguret, M., Ballard, R. D., Fox, P. J., Normark, W. R., Carranza, A., Cordoba, D. and Guerrero, J., 1980, Homogeneous Basalts from the East Pacific Rise at 21° N: Steady State Magma Reservoirs at Moderately Fast Spreading Centers, *Oceanol. Acta* **3**, 487–503.

Kappel, E. S. and Ryan, W. B. F., 1986, Volcanic Episodicity and Nonsteady State Rift Valley Along Northeast Pacific Spreading Centers: Evidence from SeaMARC I, *J. Geophys. Res.* **91**, 13925–13940.

Kappel, E. S. and Normark, W. R., 1987, Morphometric Variability within the Axial Zone of the Southern Juan de Fuca Ridge: Interpretation from SeaMARC II, SeaMARC I, and Deep-Sea Photography, *J. Geophys. Res.* **9**, 11291–11302.

Karsten, J., Hammond, S. R., Davis, E. E. and Currie, R. G., 1986, Detailed Geomorphology and Neotectonics of the Endeavour Segment, Juan de Fuca Ridge: New Results from Seabeam Swath Mapping, *J. Geophys. Res.* **97**, 213–221.

Karsten, J. L., Delaney, J. R., Rhodes, J. M. and Liias, R. A., 1990, Spatial and Temporal Evolution of Magmatic Systems Beneath the Endeavour Segment, Juan de Fuca Ridge: Tectonic and Petrologic Constraints., *J. Geophys. Res.* **95**, 19235–19256.

Kastens, K. A., Macdonald, K. C., Becker, K. and Crane, K., 1979, The Tamayo Transform Fault in the Mouth of the Gulf of California, *Mar. Geophys. Res.* **4**, 129–152.

Kastens, K. A., Ryan, W. B. F. and Fox, P. J., 1986, Structural and Volcanic Expression of a Fast-Slipping Ridge-Transform-Ridge Plate Boundary: SeaMARC I and Photographic Surveys of the Clipperton Transform Fault, *J. Geophys. Res.* **91**, 3469–3488.

Kleinrock, M. C. and Hey, R. N., 1989a, Migrating Transform Zone and Lithospheric Transfer at the Galapagos 95.5° W Propagator, *J. Geophys. Res.* **94**, 13859–13878.

Kleinrock, M. C. and Hey, R. N., 1989b1, Detailed Tectonics near the Tip of the Galapagos 95.5° W Propagator: How the Lithosphere Tears and a Spreading Axis Develops, *J. Geophys. Res.* **94**, 13801–13838.

Klitgord, K. D., 1976, Sea-floor Spreading: The Central Anomaly Magnetization High, *Earth Plan. Sci. Letts.* **29**, 201–209.

Larson, R. L., 1971, Near-Bottom Geophysical Studies of the East Pacific Rise Crest, *Geol. Soc. Am. Bull.* **82**, 823–842.

Larson, R. L., 1972, Bathymetry, Magnetic Anomalies, and Plate Tectonic History of the Mouth of the Gulf of California, *Geol. Soc. Am. Bull* **83**, 3345–3360.

Larson, R. L., Searle, R. C., Kleinrock, M. C., Schouten, H., Bird, R. T., Naar, D. F., Rusby, R. I., Hooft, E. E. and Lasthiotakis, H., 1992, Roller-Bearing Tectonic Evolution of the Juan Fernandez Microplate, *Nature* **356**, 571–576.

Lewis, B. T. R., 1979, Periodicities in Volcanism and Longitudinal Magma Flow on the East Pacific Rise at 23° N, *Geophys. Res. Letts.* **6**, 753–756.

Lewis, B. T. R., Syndsman, W. E., McClain, J. S., Holmes, M. L. and Lister, C. R. B., 1983, Site Survey Results at the Mouth of the Gulf of California, Leg 65, Deep Sea Drilling Project, *Init. Repts. DSDP* **65**, 309–318.

Lewis, B. T. R. and Robinson, P., 1983, Site 485, *Init. Repts. DSDP* **65**, 249–306.

Lonsdale, P., 1977, Structural Geomorphology of a Fast-Spreading Rise Crest: The East Pacific Rise Near 3°25′ S, *Mar. Geophys. Res.* **3**, 251–293.

Lonsdale, P., 1977b, Abyssal Pahoehoe with Lava Coils at the Galapagos Rift, *Geoology* **5**, 147–152.

Lonsdale, P. and Lawver, L., 1980, Immature Plate Boundary Zones Studied with a Submersible in the Gulf of California, *Geol. Soc. America Bull* **91**, 555–569.

Lonsdale, P. and Batiza, R., 1980, Hyaloclastite and Lava Flows on Young Seamounts Examined with a Submersible, *Geol. Soc. Am. Bull.* **91**, 545–554.

Lonsdale, P., 1985, Linear Volcanoes Along the Pacific-Cocos Plate Boundary, 9° N to the Galapagos Triple Junction, *Tectonophysics* **116**, 255–279.

Lonsdale, P., 1986, A Multibeam Reconnaissance of the Tonga Trench Axis and Its Intersection with Louisville Guyot Chain, *Mar. Geophys. Res.* **8**, 295–327.

Lonsdale, P., 1986, Tectonic and Magmatic Ridges in the Eltanin Fault System, South Pacific, *Mar. Geophys. Res.* **8**, 203–242.

Lonsdale, P., 1988, Structural Pattern of the Galapagos Microplate and Evolution of the Galapagos Triple Junctions, *J. Geophys. Res.* **93**, 13551–13574.

Londsdale, P., 1989a, Geology and Tectonic History of the Gulf of California, in *The Geology of North America,* Geological Society of America, Boulder CO, *vol. N,* pp. 499–521.

Lonsdale, P., 1989b, Segmentation of the Pacific-Nazca Spreading Center, 1° N–20° S, *J. Geophys. Res.* **94**, 12197–12225.

Lonsdale, P., 1989c, The Rise Flank Trails Left by Migrating Offsets of the Equatorial East Pacific Rise Axis, *J. Geophys. Res.* **94**, 713–743.

Lonsdale, P., 1991, Structural Patterns of the Pacific Floor Offshore of Peninsular California, *AAPG Memoir* **47**, 87–125.

Lonsdale, P., Blum, N. and Puchelt, H., 1992, The RRR Triple Junction at the Southern End of the Pacific-Cocos East Pacific Rise, *Earth Planet. Sci. Letts.* **109**, 73–85.

Lonsdale, P., 1994, Geomorphology and Structural Segmentation of the Crest of the Southern (Pacific-Antarctic) East Pacific Rise, *J. Geophys. Res.* **99**, 4683–4702.

Luyendyk, B. P. and Macdonald, K. C., 1985, A Geological Transect Across the Crest of the East Pacific Rise at 21° N Latitude Made from the Deep Submersible Alvin, *Mar. Geophys. Res.* **7**, 467–488.

Macdonald, K. C., Kastens, K., Spiess, F. N. and Miller, S. P., 1979, Deep Tow Studies of the Tamayo Transform Fault, *Mar. Geophys. Res.* **4**, 37–70.

Macdonald, K. C., Miller, S. P., Huestis, S. P. and Spiess, F. N., 1980, Three-Dimensional Modeling of a Magnetic Reversal Boundary from Inversion of Deep-Tow Measurements, *J. Geophys. Res.* **85**, 3670–3680.

Macdonald, K. C., 1982, Mid-Ocean Ridges; Fine Scale Tectonic, Volcanic and Hydrothermal Processes Within the Plate Boundary Zone, *Ann. Rev. Earth Planet. Sci.* **10**, 155–190.

Macdonald, K. C., Miller, S. P., Luyendyk, B. P., Atwater, T. M. and Shure, L., 1983, Investigation of a Vine-Matthews Magnetic Lineation from a Submersible: The Source and Character of Marine Magnetic Anomalies, *J. Geophys. Res.* **88**, 3403–3418.

Macdonald, K. C., Sempere, J. C. and Fox, P. J., 1984, East Pacific Rise from Siqueiros to Orozco Fracture Zones: Along-Strike Continuity of Axial Neovolcanic Zones and Structure and Evolution of Overlapping Spreading Centers, *J. Geophys. Res.* **89**, 6049–6069.

Macdonald, K. C. and Luyendyk, B. P., 1985, Investigation of Faulting and Abyssal Hill Formation on the Flanks of the East Pacific Rise (21° N) using Alvin, *Mar. Geophys. Res.* **7**, 515–535.

Macdonald, K. C., Fox, P. J., Perram, L. J., Eisen, M. F., Haymon, R. M., Miller, S. P., Carbotte, S. M., Cormier, M. H. and Shor, A. N., 1988, A New View of the Mid-Ocean Ridge from the Behavior of Ridge Axis Discontinuities, *Nature* **335**, 217–225.

Macdonald, K. C., Haymon, R. M., Miller, S. P., Sempere, J. C. and Fox, P. J., 1988, Deep Tow and Sea Beam Studies of Dueling Propagating Ridges on the East Pacific Rise Near 20°40′ S, *J. Geophys. Res.* **93**, 2875–2898.

Macdonald, K. C., Fox, P. J., Miller, S., Carbotte, S., Edwards, M. H., Eisen, M., Fornari, D., Perram, L., Pockalny, R., Scheirer, D., Tighe, S., Weiland, C. and Wilson, D., 1992, The East Pacific Rise and its Flanks 8–18° N: History of Segmentation, Propagation and Spreading Direction Based on SeaMARC II and Sea Beam Studies., *Mar. Geophys. Res.* **14**, 299–344.

Madsen, J. A., Forsyth, D. W. and Detrick, R. S., 1984, A New Isostatic Model for the East Pacific Rise Crest, *J. Geophys. Res.* **89**, 9997–10016.

Malahoff, A., 1984, Comparison Between Galapagos and Gorda Spreading Centers, *Proc. 13th Offshore Technology Conf.,* 115–117, Houston, Texas.

Mammerickx, J., 1980, Neogene Reorganization of Spreading between the Tamayo and the Rivera Fracture Zone, *Mar. Geophys. Res.* **4**, 305–318.

McClain, J. S. and Lewis, B. T. R., 1980, A Seismic Experiment at the Axis of the East Pacific Rise, *Mar. Geol.* **35**, 147–169.

McKenzie, D. P. and Morgan, W. J., 1969, Evolution of Triple Junctions, *Nature,* **224**, 125–133.

Menard, H. W. and Atwater, T., 1968, Changes in Direction of Sea Floor Spreading, *Nature,* **219**, 463–467.

Mitchell, N. C., 1991, Distributed Extension at the Indian Ocean Triple Junction, *J. Geophys. Res.* **96**, 8019–8043.

Ness, G. E., Sanchez, Z. O., Couch, R. W. and Yeats, R. S., 1981, Bathymetry and Crustal Ages in the Vicinity of the Mouth of the Gulf of California, Illustrated Using Deep Sea Drilling Project Leg 63 Underway Geophysical Profiles, *Initial Report of the Deep Sea Drilling Project*, **63**, 913–923, US Govt. Printing office, Washington D. C.

Ness, G. E., Lyle, M. W. and Couch, R. W., 1991, Marine Magnetic Anomalies and Oceanic Crustal Isochrons of the Gulf and Peninsular Province of the Californias, *AAPG Memoir* **47**, 47–69.

Niemitz, J. W. and Bischoff, J. L., 1981, Tectonic Elements of the Southern Part of the Gulf of California, *Geol. Soc. Am. Bull.* **92**, 360–407.

Normark, W. R., 1976, Delineation of the Main Extrusion Zone of the East Pacific Rise at 21° N, *Geology* **4**, 681–685.

Perram, L. J., Cormier, M. H. and Macdonald, K. C., 1993, Magnetic and Tectonic Studies of the Dueling Propagating Spreading Centers at 20° 40′ S on the East Pacific Rise: Evidence for Crustal Rotations, *J. Geophys. Res.* **98**, 13835–13850.

Pontoise, B., Pelletier, B., Aubouin, J., Baudry, N., Blanchet, R., Butscher, J., Chotin, P., Diament, M., Dupont, J., Essen, J., Ferriere, J., Herzer, R., Lapouille, A., Louat, R., Ozouville, L., Soakai, S. and Stevenson, A., 1986, La Subduction de la Ridge de Louisville le Long de la Fosse des Tonga, *Comptes Rendus Acad. Sci. Paris* **303**, 911–918.

Rangin, C. and Francheteau, J., 1981, Fine-Scale Morphological and Structural Analysis of the East Pacific Rise, 21° N (Rita Project), *Oceanol. Acta* **3**, 15–24.

Reid, I., Orcutt, J. and Prothero, W., 1977, Seismic Evidence for a Narrow Zone of Partial Melting Underlying the East Pacific Rise at 21° N, *Geol. Soc. Am. Bull.* **88**, 679–682.

Renard, V. and Allenou, J. P., 1979, Sea Beam, Multi-Beam Echo-Sounding in "Jean Charcot", *Int. Hydrog. Rev.* **56**, 35–67.

Riddihough, R., 1984, Recent Movements of the Juan de Fuca Plate System, *J. Geophys. Res.* **89**, 6980–6994.

Rubin, A. M. and Pollard, D. D., 1988, Dike-Induced Faulting in Rift Zones of Iceland and Afar, *Geology* **16**, 413–417.

Schilling, J. G., Kingsley, R. H. and Devine, J. D., 1982, Galapagos Hot Spot-Spreading Center System. 1. Spatial Petrological and Geochemical Variations (83° W–101° W), *J. Geophys. Res.* **87**, 5593–5610.

Schouten, H. and White, R. S. 1980, Zero-Offset Fracture Zones, *Geology* **8**, 175–179.

Schouten, H., Klitgord, K. D. and Gallo, D. G., 1993, Edge-Driven Microplate Kinematics, *J. Geophys. Res.* **98**, 6689–6701.

Searle, R. C. and Hey, R. N., 1983, GLORIA Observations of the Propagating Rift at 95.5° W on the Cocos-Nazca Spreading Center, *J. Geophys. Res.* **88**, 6433–6447.

Shoberg, T., Stein, S. and Karstens, J., 1991, Contraints on Rift Propagation History at the Cobb Offset, Juan de Fuca Ridge, from Numerical Modeling of Tectonic Fabric, *Tectonophysics* **197**, 295–308.

Small, C. and Sandwell, D. T., 1989, An Abrupt Change in Ridge Axis Gravity with Spreading Rate, *J. Geophys. Res.* **94**, 17383–17392.

Smith, D. K. and Cann, J. R., 1992, The Role of Seamount Volcanism in Crustal Construction at the Mid-Atlantic Ridge (24°–30° N), *J. Geophys. Res.* **97**, 1645–1658.

Spiess, F. N., Macdonald, K. C., Atwater, T., Ballard, R., Carranza, A., Cordoba, D., Cox, C., DiazGarcia, V., Francheteau, J., Guerrero, J., Hawkins, J., Haymon, R., Hessler, R., Juteau, T., Kastner, M., Larson, R., Luyendyk, B., Macdougall, J., Miller, S., Normark, W., Orcutt, J. and Rangin, S., 1980, East Pacific Rise: Hot Springs and Geophysical Experiments, *Science* **207**, 1421–1433.

Sykes, L. R., 1970, Focal Mechanisms Solutioons for Earthquakes Along the World Rift System, *Seismol. Soc. Am. Bull.* **60**, 1749–1752.

van Andel, T. H. and Ballard R. D., 1979, The Galapagos Rift at 86° W; 2, Volcanism, Structure, and Evolution of the Rift, *J. Geophys. Res.* **84**, 5390–5406.

Wang, X. and Cochran, J. R., 1993, Gravity Anomalies, Isostasy, and Mantle Flow at the East Pacific Rise Crest, *J. Geophys. Res.* **98**, 19505–19531.

Wetzel, L. R., Wiens, D. A. and Kleinrock, M. C., 1993, Evidence from Earthquakes for Bookshelf Faulting at Large Non-Transform Ridge Offsets, *Nature* **362**, 235–237.

Wilson, D. S., 1989, Deformation of the So-Called Gorda Plate, *J. Geophys. Res.* **94**, 3065–3075.

Wilson, D. S., 1990, Kinematics of Overlapping Rift Propagation with Cyclic Rift Failure, *Earth Planet. Sci. Letts.* **96**, 384–392.